Fluorescent Probes as Reporters on the Local Structure and Dynamics in Sol−Gel-Derived Nanocomposite Materials

Tracey Keeling-Tucker and John D. Brennan*

Department of Chemistry, McMaster University, Hamilton, Ontario L8S 4M1, Canada

Received February 2, 2001. Revised Manuscript Received May 12, 2001

The use of steady-state and time-resolved fluorescence spectroscopy to probe the internal microenvironment of sol−gel-derived organic−inorganic nanocomposites formed from alkoxysilane precursors is reviewed. The review focuses on the use of small organic probes and fluorescent biomolecules that provide information on pore−solvent composition and polarity, internal solvent and dopant dynamics, environmental heterogeneity and phase segregation, and surface chemistry, as determined by molecule−matrix interactions. Emphasis is placed on advanced fluorescence methods that can provide unique information on sol−gel-derived composite materials. The discussion begins with a description of the different fluorescent probes that have been used to study sol−gel materials. The application of fluorescence methods to examine Class I and Class II hybrid materials is then described, highlighting the specific information available from different probes and the methods used to obtain information on the structure and dynamics of such materials. This section highlights the overall effects of dispersed and bound organic dopants on the polarity, dynamics, heterogeneity, and surface chemistry of nanocomposites. Finally, fluorescence studies on emerging materials, including templated nanocomposites and biomaterials, are described, and the overall utility of fluorescence spectroscopy for probing of such materials is discussed.

1. Introduction

The development of nanocomposites having properties that are intermediate between those of organic and inorganic materials has been an area of intense interest in the past decade. Such materials find applications in areas such as the development of photonic devices,[1] microelectronics,[2] solid-phase microextraction coatings,[3] and chemical sensors.[4] One of the prevalent methods for forming such materials has been through the use of a low-temperature sol−gel polymerization route wherein a metal alkoxide precursor undergoes hydrolysis and condensation reactions to form a highly cross-linked solid.[5,6] Such materials can be prepared as powders, fibers, thin films, or bulk materials of virtually any shape and size. Furthermore, the use of low-temperature processing conditions allows for the encapsulation of a variety of dopants including organic, organometallic, and biological molecules.[7] Adding organically modified metal alkoxides or organic polymer dopants to the sol before gelation allows one to prepare organic−inorganic nanocomposite materials with a high degree of control over the final properties of the material (i.e., polarity, homogeneity, surface chemistry, pore size, etc.).[8]

Key considerations in preparing sol−gel-derived nanocomposites are the distribution of the dopants and additives and the nature of the local microenvironment(s) within the material, particularly if one wishes to encapsulate an organic or biological dopant to create a photonic device or sensor. It is well-known that the evolution of a sol−gel-derived material is kinetically controlled and thus continues long after gelation has occurred. It is also known that both preparation and aging conditions (i.e., precursors, catalysts, H_2O:Si ratio, pH, temperature, dopant level, etc.) will influence the physicochemical properties of the resulting solid material.[5]

A derived variety of methods have been used to study sol−gel materials, including ^{13}C and ^{29}Si NMR,[9] infrared,[10] and Raman spectroscopies,[11] cryogenic gas adsorption analysis,[12] and small-angle X-ray scattering.[13] However, these methods generally report on average properties for the bulk material and are relatively insensitive to local conditions surrounding dopant molecules. Thus alternative methods are needed to assess the materials at the molecular level.

The nature of the local microenvironment(s) within a sol−gel-derived nanocomposite is an important factor in designing materials for sensing or photonic applications. For example, factors such as microscopic phase separation can dramatically alter the behavior of dopants within a nanocomposite. Furthermore, the environment experienced by the dopant (i.e., polarity, local microviscosity, interactions with pore walls, and preferential partitioning into a given phase) will have an impact on the dynamics, stability, and accessibility of the dopant and as such may lead to unwanted material properties. The need to understand the nature of the local microenvironments within nanocomposites requires a method that is sensitive to phenomena occurring at the molecular scale. In these instances fluorescence spectroscopy is the method of choice as it reports on the local microenvironment surrounding a probe molecule.[14]

* To whom correspondence should be addressed. Tel.: (905) 525-9140 (ext. 27033). Fax: (905) 522-2509. E-mail: brennanj@mcmaster.ca. Internet: http://www.chemistry.mcmaster.ca/faculty/brennan.

10.1021/cm010119m CCC: $20.00
Published on Web 07/31/2001

Table 1. Fluorescent Parameters Used To Monitor Sol−Gel-Derived Nanocomposite Materials

parameter	uses	refs
steady-state intensity	probe concentration	77
	pH	59
	leaching	79
emission wavelength	internal polarity	22, 23, 33−35, 47, 48, 53, 55, 62, 63
	surface silanol content	23, 33, 55
	solvent composition, pH	23b, 41, 72, 73
emission spectral width	environmental heterogeneity	23b, 33
red-edge excitation studies	solvent rigidity	51
steady-state rotational anisotropy	surfactant mobility in films	73−76
	orientation of probes	76
	viscosity	22, 27a, 32, 41, 81a
decay of intensity (lifetime)	solvent rigidity	61, 62
distributed lifetime analysis	environmental heterogeneity	48
stretched exponential lifetimes	dimensionality of material	60, 69, 70
time-resolved anisotropy decay	distributions of environments	22
	microviscosity	27a, 32, 53
	probe−silica interactions	62, 84, 85, 86
resonance energy transfer	pore dimensions and smoothness	26
quenching of fluorescence	probe accessibility	44, 47, 53, 86, 87
	translational mobility	81a
excimer formation	conformational flexibility	50, 71, 74
	local concentration of probes	47, 69, 70, 77

Fluorescent probes can be incorporated into sol−gel-derived materials at very low levels ($<10^{-6}$ M) and thus do not alter the overall properties of the material. Fluorescent probes can also be introduced into the material either as a dispersed dopant or as part of the silica network via covalent attachment, thereby sensing different regions of the material. Furthermore, the probe may be bound to or intrinsically part of an entrapped biomolecule, allowing for studies of biomolecule conformation, accessibility, and dynamics within biologically active nanocomposite biomaterials. In all cases, the combination of steady-state and time-resolved fluorescence techniques makes it is possible to not only determine the average microenvironment of a probe but to also ascertain the distribution of unique microenvironments within a material and how this is affected by processing conditions.

In this paper we review the use of fluorescence spectroscopy for probing the internal microenvironments within sol−gel-derived nanocomposites formed from alkoxysilane precursors and containing either dispersed or covalently attached organic moieties, or biomolecules. We begin with a brief overview of the various fluorescent probes that have been utilized to examine sol−gel-derived nanocomposites, highlighting the information on the material properties that can be extracted from the fluorescence probes. The application of fluorescence spectroscopy to characterize Class I and Class II hybrid materials is then reviewed with an emphasis on how different additives and processing conditions modulate the internal microenvironment of the nanocomposite and how this in turn alters the overall material properties. Fluorescence studies on emerging materials, including templated nanocomposites and biomaterials, are then described, with emphasis on the insights that fluorescence spectroscopy can provide on such materials. We conclude by presenting an overview of the current understanding of sol−gel-derived nanocomposites as derived from fluorescence measurements and discuss the future of the technique for studying nanocomposites.

2. Background to Fluorescence Techniques

The fluorescence emission process has been known for well over a century since initially discovered by Stokes,[15] and the theoretical and practical aspects of fluorescence spectroscopy have been described thoroughly in a number of excellent texts.[16−20] In general, the fluorescence emission of probes within sol−gel-derived materials is relatively complex because the excited molecule can have a variety of interactions with its local microenvironment (solvent dipolar relaxation, collisions with solvent and other molecules, rotational motions, protonation, tautomerization, etc.). Thus, the intensity, energy, decay time, and polarization of the emitted radiation are extremely sensitive to the local microenvironment surrounding the probe. Both steady-state and time-resolved fluorescence measurements can be used to characterize sol−gel-derived nanocomposites. The information derived from steady-state experiments is averaged over all microenvironments and generally provides only a small amount of the total information that is available from the decay process. The use of time-resolved fluorescence to probe the microenvironments of sol−gel-derived materials allows one to determine the underlying components that contribute to the average signal and hence provides information on both the nature and proportional occupation of probes within the different microenvironments.[14]

Table 1 summarizes the various fluorescence measurement methods that have been used to examine sol−gel-derived materials. The material properties that can be examined include solvent composition, pH and polarity, rotational and diffusional mobility of species in the matrix, homogeneity of the internal environment, accessibility of species to external reagents, and the surface chemistry of the silica material. The specific information that is obtained depends on the measurement technique employed (steady-state or time-resolved detection) and the type of experiment performed (i.e., quenching, energy transfer, or depolarization). By combining multiple measurement techniques, a detailed picture of the molecular-scale structure and dynamics of sol−gel-derived materials emerges, allowing for new insights into the effects of precursors, additives, processing, and aging methods of the properties of the final material, as discussed in detail below.

3. Fluorescent Probes of Sol−Gel Materials

The selection of a fluorescent probe to characterize a sol−gel-derived material is perhaps the most critical factor for determining the type and quality of information obtained and thus warrants special attention. A

wide variety of fluorescent probes exist and typically fall into various classes such as pH-sensitive probes, solvatochromic probes, rigidochromic probes, anisotropy probes, and so on.[21] These tend to be incorporated into the materials during the early stages of the sol−gel process when the hydrolyzed precursor and entrapped molecule(s) are mixed and allowed to gel. During the subsequent condensation reactions the probe molecules become entrapped within the pores as the material forms and may become part of the matrix network. As outlined in the review by Dunn and Zink,[14] the probe may exist in one or more different environments within the matrix: the liquid-filled pore, the interfacial region between the liquid and the pore wall (effectively a boundary layer of solvent a few molecules thick), adsorbed on the pore wall or constrained within a channel between pores. Furthermore, in the case of nanocomposites, the probe may associate with either the organic or inorganic (silica) subphase or may reside at the interface between two phases and may assume a specific orientation within the material depending on the nature of the different phases (see section 6A). Hence, the specific probe chosen for examination of the internal environment is of critical importance, as different probes will report from different locations.

In this review, we consider two types of probes. We first consider the information provided by small organic molecules, which are by far the most widely used species for probing nanocomposite materials. We then review the information that can be obtained from large fluorescent biomolecules entrapped in biologically active nanocomposites (section 6B), with emphasis on emerging methods to control biomolecule behavior by manipulating biomolecule−silica interactions. Table 2 provides a listing of the various small organic probes that have been used to examine sol−gel-derived nanocomposites, along with the information that can be obtained from the probe. In general, information on structure and dynamics may be obtained from the organic phase using hydrophobic probes, from the silica phase using charged or hydrophilic probes and from interfacial regions using amphiphilic probes. Furthermore, one can choose between a dispersed probe or one that is covalently attached to the silica network using organosilane precursors of the type $R'_nSi(OR)_{4-n}$, where R′ is the fluorescent moiety. In such cases, the probes are constrained to the region close to the pore wall and can provide unique insights into the surface chemistry and mobility of sol−gel-derived materials. In addition, the location of the probe can, in some cases, be controlled using molecular templating methods (see section 6A), allowing for specific probing of a given subphase in a mesostructured nanocomposite. In the remaining sections, the information provided by fluorescence probes is reviewed for various types of sol−gel-derived nanocomposites. Emphasis is placed on understanding (1) the location of the probe, (2) the origin of the fluorescence signal (which is important in interpreting the results in a meaningful way), (3) the evolution of the molecular-scale structure and dynamics of the materials, and (4) the overall effect of adding dopants and organosilanes on the material properties.

Table 2. Fluorescent Probes Utilized in the Study of Sol−Gel-Derived Nanocomposites

probe	uses	refs
7-azaindole (7AI)	polarity, homogeneity, and surface silanol content	23a, 23b,33, 55
1-bromo-4-(bromo-acetyl)naphthalene	surfactant mobility	74
dansyl	polarity, viscosity	48, 51
	protein accessibility	86
2,6-diamidino-2-phenylindole (DAPI)	accessibility of cells	75
1,1′,3,3,3′,3′-hexamethylindotricarbocyanine iodide (HITC)	solvent rigidity	61
oxazine-1	polarity, viscosity	62
fluorescein	pH, polarity, leaching	79
	protein accessibility	87
fluorescein−dextran	pH, mobility	59
ketocyanine dye	polarity	35
prodan	polarity, homogeneity	22, 33, 55
	microviscosity	22, 49, 74
pyranine	pH, alcohol/water ratio	23b, 41, 72, 73
	mobility	73
pyrene	polarity	32, 34, 47, 53, 63
	surfactant concentration	63, 71, 73, 74
	accessibility	47, 53
	molecular imprinting	77
pyrene-labeled liposomes	entrapped liposome behavior	78
1,12-bis(1-pyrenyl) dodecane	mobility	50
pyrene-coumarin 153	mobility in hydrophobic regions of glass	60, 69, 70
2-p-toluidinyl naphthalene-6-sulfonate (2,6-TNS)	mobility in thin films	71
$Ru(bpy)_2^{2+}$-methyl viologen	mobility in polar regions of glass	69, 70
	mobility of entrapped solvent	
rhodamine 6G		32, 53
ruthenium complexes	accessibility to O_2	44
	development of matrix	76
ClRe(CO)3-2-2′-bipyridine	solvent motions	25
Eu(III)	molecular templating	76

4. Preparation of Nanocomposites by the Sol−Gel Method

Scheme 1 shows a general approach for preparing organic−inorganic nanocomposite materials by the sol−gel process. The preparation of nanocomposite materials by this route makes use of mixtures of organic and inorganic metal alkoxides of the general form $M(OR)_4$, $R'_nM(OR)_{4-n}$, or $R'R''M(OR)_2$, where M is typically Si, Al, or Ti, and the R groups may be aromatic or aliphatic. These species are generally hydrolyzed under acidic or basic conditions, either separately or together, and can have other organic additives, such as polymers or surfactants, or biomolecules, such as proteins, peptides, or nucleic acids, dispersed into the matrix before gelation occurs. The gelation can be done at the pH of hydrolysis, or a buffer may be added (usually containing the dopants and biomolecule) to accelerate the gelation process. Upon gelation, a solid material is produced, the nature of which depends on several parameters, including the type and level of precursors and additives, solution pH, H_2O:Si ratio, and cosolvents.[5−7] Following gelation, the materials are generally aged for periods of up to several months in air or water and may also be heated to accelerate the aging process. Thus, a wide variety of final materials is possible depending on the specific conditions used for hydrolysis, gelation, and aging.

As indicated in Scheme 1, the types of materials that can be formed by the sol−gel process fall into four general classes; (1) purely inorganic materials derived solely from tetraalkoxysilanes, (2) materials with dis-

Scheme 1. General Approach for Preparing Organic−Inorganic Nanocomposite Materials by the Sol−Gel Process Using Organosilane Precursors and Dispersed Organic Additives

$$Si(OR)_4 + R'_nSi(OR)_{4-n} + H_2O + H^+ \rightarrow Si(OR)_{4-n}(OH)_n + R'_nSi(OR)_{4-n-m}(OH)_m + m\ ROH$$

(Hydrolysis)

a) $2\ Si(OEt)_{4-n}(OH)_n \rightarrow (OH)_{n-1}(OEt)_{4-n}Si\text{-}O\text{-}Si(OEt)_{4-n}(OH)_n + H_2O$

b) $2\ R'_nSi(OR)_{4-n-m}(OH)_m \rightarrow (OH)_{m-1}(OR)_{4-n-m}R'_nSi\text{-}O\text{-}SiR'_n(OEt)_{4-n-m}(OH)_{m-1} + H_2O$

c) $Si(OR)_{4-n}(OH)_n + R'_nSi(OR)_{4-n-m}(OH)_m \rightarrow (OH)_{n-1}(OR)_{4-n}Si\text{-}O\text{-}SiR'_n(OEt)_{4-n-m}(OH)_{m-1} + H_2O$

(Homo and Hetero Condensation)

Homo and hetero oligomers + additive (+ biomolecule) $\rightarrow R'_nSi\text{-}O_{(2-1/2n)}$ •additive(•biomolecule)

(additive = polymer, surfactant, polyelectrolyte, etc) (Gelation/Aging/Drying)

persed organic dopants (referred to as Class I materials), (3) materials with covalently attached organic groups (referred to as Class II materials), and (4) hybrid Class I/II materials with both covalently attached and dispersed organic species present in the matrix. Furthermore, the use of self-assembled structures as templates to form the organic phase can result in the production of mesostructured materials with unique lamellar, hexagonal, or cubic structures. In addition, these materials can be prepared with an entrapped biomolecule, leading to different classes of biomaterial. Given that fluorescence studies of inorganic silicates has been recently reviewed,[14] our review will focus primarily on fluorescence studies of Class I and Class II nanocomposite silicas, templated nanocomposites, and biologically active nanocomposites. In the case of biomolecule-doped nanocomposites, we consider biomolecules in pure silica to be a nanocomposite because the material can be thought of as a Class I nanocomposite with a dispersed biological polymer; hence, these materials are also reviewed.

5. Fluorescence Studies of Nanocomposite Materials

A. Materials with Covalently Attached Organic Functionalities (Class II Materials). Nanocomposite materials are formed by adding an organic moiety to a silicate glass (either covalently or by dispersion) as a means of altering one or more of the properties of the silica. Numerous fluorescence studies of pure silica materials[14] have shown that such materials tend to (a) be relatively polar owing to exposed silanol groups,[22,23] (b) have high surface charge owing to high siloxide levels at neutral pH,[5] (c) have relatively rigid solvent phases (likely owing to adsorption of the solvent to the pore wall),[24,25] (d) be heterogeneous in terms of pore size,[26] mobility,[27] and polarity[28] (as determined by distributions of fluorescence lifetimes and rotational correlation times), (e) have significant inaccessible fractions,[29] and (f) contain sufficiently large pores to allow encapsulated molecules to retain a reasonable degree of translational mobility.[30] A key problem with pure silica materials is that control over the final properties and the final location of the probe is relatively limited, mainly being achieved through manipulation of pH, H_2O:Si ratio, and drying conditions. Thus, the addition of organic species (such as alkylsilanes, polymers, or surfactants) opens a new route to control material properties.

One method of modifying the properties of a sol−gel-derived glass is the production of materials wherein the organic species is covalently attached to the silica matrix (Class II material). A variety of organosilanes have been used to form these materials, as summarized in Table 3. In most cases, the organically modified silane is added to tetraethyl orthosilicate (TEOS) or tetramethyl orthosilicate (TMOS), although some materials have been derived using the organosilane as the sole precursor. The methodology behind various synthetic methods to produce such glasses is discussed in detail by Schubert et al.[8] and Avnir et al.[31] and thus will not be discussed in detail here.

Table 3. Organosilane Species Used for the Preparation of Class II Nanocomposite Materials That Have Been Studied by Fluorescence Methods

ormosil	refs
(aminopropyl)triethoxysilane	77
N,*N*-bis(triethoxysilanepropyl)-2,6-pyridine dicarboximide	76
triethoxysilane	34
methyltrimethoxysilane	47
methyltriethoxysilane	32, 33, 41, 55
ethyltrimethoxysilane	47
ethyltriethoxysilane	32
allyltriethoxysilane	32
propyltrimethoxysilane	33
n-hexyltrimethoxysilane	47
n-hexadecyltrimethoxysilane	47
n-octyltriethoxysilane	32, 41
dimethyldimethoxysilane	35, 55
dimethyldiethoxysilane	32
diethyldiethoxysilane	32
phenyltrimethoxysilane	35, 41, 47
diphenyldimethoxysilane	35
dansyltriethoxysilane	48
(1-pyrenylmethyl)trimethoxysilane	47
1,12-bis(1-pyrenyl)dodecane	50
poly(propylene oxide)bis-silane precursor	60
poly(ethylene oxide)bis-silane precursor	60

Several papers have described fluorescence probing of organically modified silica (ORMOSIL) materials. The key properties that have been examined by this method are polarity, mobility, accessibility, and pore structure. Several other studies have aimed to compare the differences in probe environment for attached versus dispersed probes. The general tendency when creating these materials is to cohydrolyze the organosilane precursor together with a tetraalkoxysilane to form the ORMOSIL, and thus all samples described below refer to materials derived from cohydrolyzed silane mixtures, unless otherwise stated. A brief review of the various fluorescence studies of Class II materials follows.

Polarity. Studies of polarity of ORMOSIL materials have primarily considered the evolution of solvent polarity[32,33] and the effect of the organic group on the final emission properties of the entrapped dye.[32−35] In an early study, Matsui used pyrene fluorescence to

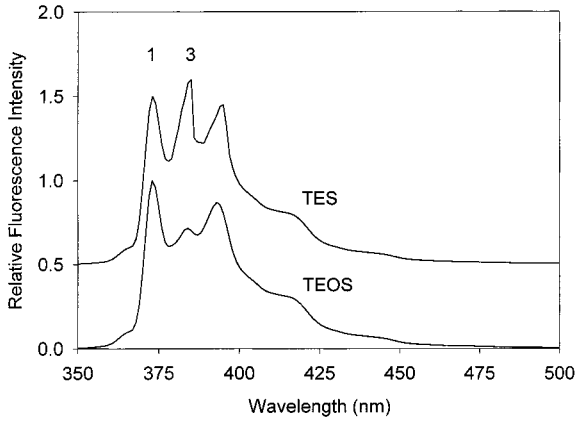

Figure 1. Changes in pyrene I_1/I_3 emission ratios as a function of the polarity of sol−gel-derived nanocomposites. The lower spectrum shows the emission spectrum of pyrene in a TEOS-derived glass, while the upper spectrum shows the spectrum in a triethoxysilane-derived glass. The ratio of intensities for peaks 1 and 3 (I_1/I_3) clearly decreases as the sample becomes less polar (adapted from ref 34).

examine the effect of adding triethoxysilane (TES) to TEOS at varying proportions to form glasses.[34] The environment surrounding this probe perturbs the symmetry of its π-electron orbitals owing to Herzberg−Teller symmetry distortions, altering the vibronic coupling between the $B^2{}_u$ and $B^1{}_u$ states.[36] This enhances the forbidden transition from the $B^2{}_u$ excited state, resulting in enhanced emission from the I_1 band at 373 nm as the local dipolarity increases. This is usually measured relative to the I_3 band at 393 nm, leading to higher I_1/I_3 ratios as solvent dipolarity increases.[37] The I_1/I_3 ratio suggested that the material initially exhibited similar internal environments, regardless of the amount of TES added, owing to similarities in the composition of the entrapped solvent. However, as drying proceeded, the emission of the pyrene shifted to reflect a more hydrophobic environment, which increased in hydrophobicity as the amount of TES increased, as shown in Figure 1. The results were ascribed to a reduction in the amount of SiOH and adsorbed water on the pore wall, owing to the presence of the nonreactive silane site, indicating that pyrene reported on the pore wall composition rather than the solvent once the materials were aged.

Later studies with pyrene have expanded the types of ORMOSILS to include those with methyl, dimethyl, ethyl, diethyl, octyl, and allyl groups.[32] Once again it was observed that increased levels of organic groups produced more hydrophobic materials. However, these studies also showed a rather interesting trend wherein dialkyl silanes, such as dimethlydiethoxysilane (DMDES) or diethlydiethoxysilane (DEDES), produced larger shifts in polarity than similar amounts of long-chain organosilanes, such as octyltriethoxysilane (OTES). These results suggest that the number of alkyl chains is a more important factor that the length of the alkyl chain in determining overall polarity of the glass.

Our group has used 7-azaindole (7AI) and 6-propionyl-2-dimethylamino(naphthalene) (PRODAN) fluorescence to examine ORMOSILS containing up to 20% (v/v) of methyltriethoxysilane (MTES) or 10% (v/v) of dimethyldimethoxysilane (DMDMS).[33] PRODAN is extremely solvatochromic[38] and thus shows large shifts in emission

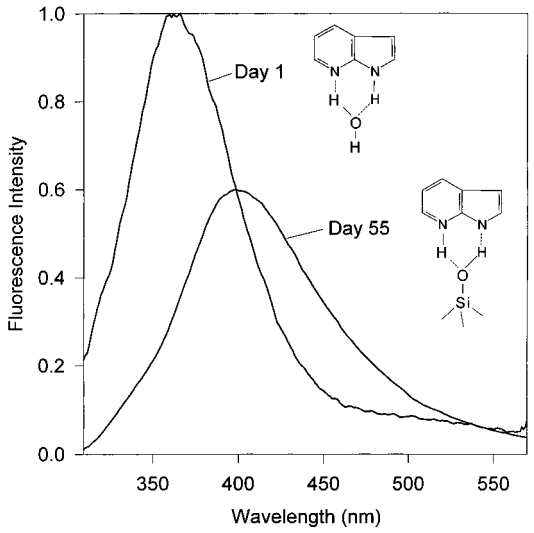

Figure 2. Emission spectra of 7-azaindole at early and late stages in the evolution of a TEOS-derived material. At early times, the emission is dominated by probe−solvent interactions (Day 1), while at later times (Day 55) the probe adsorbs to the silanol groups on the silica surface, resulting in an excited-state proton-transfer reaction to produce emission at 420 nm (adapted from ref 23b).

wavelength with local dipolarity. 7AI is also strongly solvatochromic and thus shows shifts in emission maxima with solvent polarity.[39] Furthermore, in the case of 7AI, it is known that the excited probe can undergo both protonation and tautomerization reactions in the presence of protic media,[39] producing unique emission properties in each case. In 1989, Matsui et al.[23a] demonstrated that 7AI undergoes a significant shift in fluorescent emission wavelength, owing to specific interactions of the probe with silanol groups on the silica, as shown in Figure 2. A unique emission maximum at ≈420 nm, consistent with strong hydrogen bonding to the pyridine nitrogen, is thus observed in sol−gel glasses, owing to the adsorption of the probe onto surface silanols.

Studies involving 7AI and PRODAN indicated that immediately after gelation and up to ≈5−7 days, the internal polarity of materials was dominated by the solvent composition and evolved in a manner similar to that for purely inorganic materials.[14] However, a point was reached where the solubility of the probe was exceeded (owing to solvent loss), and at this point the polarity of the organosilane dopants within the binary composites began to take over, consistent with partitioning of the probes to hydrophobic sites on the pore walls. Increased levels of MTES or DMDMS were able to produce a more hydrophobic environment, producing a smooth change in polarity with concentration of organosilane (indicative of good dispersion of the organosilane). An interesting observation from this study was that washing of materials just following gelation to remove the entrapped alcohol resulted in much more narrow spectral fwhm values, indicative of a more homogeneous distribution of probe environments. It was also noted that the homogeneity was greatly improved if components were cohydrolyzed rather than separately hydrolyzed and mixed. The results suggest that higher levels of water at early times result in a repartitioning of the sparingly soluble probes into regions of high

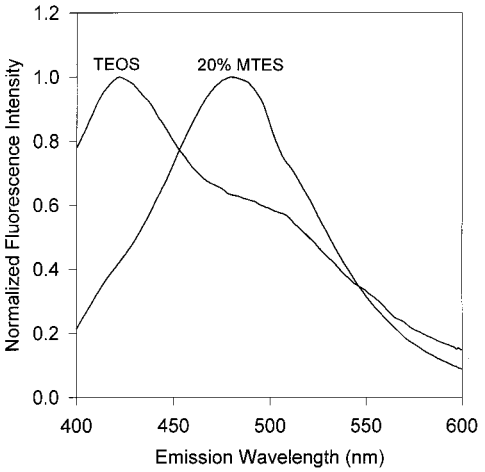

Figure 3. Typical PRODAN emission spectra in sol−gel-processed glasses derived from TEOS with and without 20% MTES after 80 days of aging (adapted from ref 33).

ORMOSIL content so that all probes sense similar environments during the evolution of the material.

An interesting finding from this study was that the emission of PRODAN showed two distinct peaks in the more polar glasses, with a new peak at 430 nm growing in intensity as polar materials aged.[33] This feature is illustrated in Figure 3, which shows the typical PRODAN spectra in neat TEOS and samples containing 20% MTES after 80 days of aging. The origin of the peak at 430 nm has been attributed to the aggregation of the probe,[40] which occurs as the water is expelled from the matrix. In the absence of organosilane moieties, the pore surface is too polar to associate with the hydrophobic probe; thus, self-association of probes occurs. Inclusion of the organosilane results in solubilization of the probe, owing to preferential partitioning of the probe into the organic regions of the matrix, thus removing the aggregate peak. Hence, the ratio of the peaks at 430/≈480 nm can be used to assess both the solubility of the probe within the matrix (indirectly reporting on solvent composition) and the polarity in the region of the pore wall.

Pyranine (8-hydroxyl-1,3,6-trisulfonated pyrene) has also been used by Wittouck and co-workers[41] to monitor the solvent composition in the Class II nanocomposite materials. This probe is sensitive to excited-state proton-transfer phenomena[42] and as a result it emits at two wavelengths corresponding to the protonated and deprotonated forms of the probe. Ratiometric comparison of the fluorescence emission intensities of the blue (438 nm) and green (515 nm) peaks of the pyranine emission spectrum can be used to quantify the relative concentrations of alcohol and water in the matrix pores, as has been demonstrated for a variety of sol−gel-derived bulk materials.[14,43] Wittouck et al.[41] found that curing of TEOS and TEOS/ORMOSIL films for 30 min at 160 °C eliminated all solvent from the pores, thereby forcing all probe molecules to interact with the siloxane network itself. In both heated and nonheated samples, gradually increasing the amount of phenyltriethoxysilane (PhTES), MTES, or octyltriethoxysilane (OTES) at the expense of TEOS resulted in a more nonpolar environment, consistent with the organically modified silane coating the pore wall.

Lobnik and Wolfbeis have also used fluorescence to determine the polarity within sol−gel materials that were derived from various proportions of TMOS with MTMS, PhTES, DMDMS, or diphenyldimethoxysilane.[35] In this case, both the fluorescence intensity and the emission maximum of the polarity sensitive probe, ketocyanine (KC) was examined and, in agreement with other studies, the incorporation of organic functionality into the matrix imparted an increased degree of hydrophobicity into the material. However, broad excitation profiles were also obtained from these materials, which suggested that lower concentrations of organosilane, compared to TMOS, resulted in discrete microdomains of differing polarity within the material, with the probe associating with both polar and nonpolar regions. In contrast, a more homogeneous environment was observed with higher fractions of organosilane (50% or more), suggesting that at higher levels, the organosilane was able to disperse throughout the material. This was an important finding because it indicated that the level of organosilane could be manipulated to control both polarity and homogeneity within the materials.

Mobility. A key consideration in the development of nanocomposite materials is the rotational and translational mobility of molecules within the matrix. This is particularly important in cases where the materials are used for sensors, bioreactors, or drug delivery vehicles. The rotational mobility of dopants is usually assessed by using fluorescence anisotropy experiments.[22] In this method, the sample is excited with vertically polarized light, and the emission intensity is recorded using vertical and horizontal emission polarizer settings. The fluorescence anisotropy, which is related to the difference in the intensity of vertically and horizontally polarized emission, increases as the probe becomes less mobile.[16] As discussed in the review by Dunn and Zink,[14] the mobility of a fluorescent probe in a sol−gel-derived material generally reports on both solvent motion and on association of the probe with the pore wall. In nanocomposite materials, the hydrophobic probes would be expected to report predominantly on solvent mobility only at early stages. Following sufficient loss of solvent, the probe would be expected to partition into the organic phase; thus, the mobility information is generally localized in this phase and, thus, gives information on the mobility of the alkyl chains within the matrix.

Bright and co-workers have used R6G to probe the rotational mobility within organosilane-derived nanocomposites.[32] Their study showed that the rotational mobility of the probe increased as the organosilane was incorporated. This probe is positively charged and, thus, would be expected to associate with the negatively charged silica surface in pore silica materials. Increased levels of organosilane cause the probe to preferentially associate with the organic phase. The higher mobility as organosilane content increased therefore suggests that the alkyl chains are mobile within the matrix, thus providing a more dynamic internal environment. This result is supported by the work of Wittouck et al.[41] who showed that the emission anisotropy of pyranine decreased upon addition of organosilanes, reflecting higher mobility in ORMOSILS relative to that in TEOS-derived materials. This result was attributed to a decrease in

network connectivity (and thus larger pores), but likely also reflects less adsorption of the charged probe to the rigid silica portions of the pore walls. Such a result is consistent with the alkyl chains of the organic dopants remaining accessible to the probes (i.e., not incorporated within the silica matrix) and, thus, modifying the properties of the solvent−silica interface.

The translational mobility of small molecules in ORMOSILS and their ability to enter the material and interact with an entrapped dopant have also been investigated. Such studies provide information on the mobility of species within the solvent phase of nanocomposite materials and also provide insight into preferential partitioning of external reagents into the materials, owing to microextraction phenomena. MacCraith and co-workers have compared the O_2 quenching of Ru(II) dyes within TEOS and MTES films.[44] In these studies, MTES led to enhanced sensitivity to O_2, which was attributed to preconcentration of O_2 into the glass via a solid-phase microextraction process. On the other hand, Murtagh observed somewhat poorer O_2 quenching efficiencies for Ru(II) species present in glasses containing low levels of MTMS doped into TEOS.[45] This was assumed to be due to partitioning of the charged probe into the more polar TEOS phase, while O_2 partitioned into the organic phase. Overall, these studies indicate that the location of the fluorescent probe varies significantly in response to variations in organosilane levels. Hence, organic doping must be carefully controlled to achieve a desired set of properties for ORMOSILs such that hydrophobic character is imparted while avoiding phase segregation and loss of control over probe location.

Zhang and Wang used sulfosalicylic acid emission to examine the mobility within nanocomposites composed of the covalent dopant γ-glycidoxypropyltrimethoxysilane (GPTMS) dispersed within PMMA-doped glasses.[46] In this case, the glycidoxy group can form covalent bonds with the polymer, producing a covalently bonded polymer phase. It was found that the luminescence and photodecay of the probe was unaffected when the polymer was dispersed in the silica without GPTMS, but that adding GPTMS at a level of 20 mol % produced substantial improvements in luminescence intensity and photostability, consistent with low mobility of the probe and poor accessibility to oxygen. It was postulated that the use of the GPTMS allowed covalent bridges to form between the organic and inorganic phases and produced a much tougher material that was more rigid and provided better protection of the fluorophore from the external environment.

Bound Probes. One area that is receiving increased attention is the photophysical behavior of probes that are bound to the silica matrix. By covalently bonding the probe to the glass, the potential for leaching of the probe is removed, making for more stable photonic and sensor devices. However, attachment of the probe also constrains the probe to the solvent−silica interface and thus alters its local microenvironment, mobility, and response to external reagents.

An early study aimed at understanding the differences in the environments of bound and dispersed probes utilized the emission of pyrene that was dispersed or covalently bonded (using 1-(pyrenylmethyl)-trimethoxysilane) into sol−gel-derived nanocomposite materials formed from TEOS mixed with methyl, ethyl, phenyl, hexyl, or hexadecyl trimethoxysilanes.[47] Both the free molecule and the attached pyrene probe were found to be well-dispersed in the matrix, showing little or no excimer emission after aging of the matrix. Furthermore, both species detected similar changes in the polarity of the microenvironment arising from incorporation of organosilane precursors. Perhaps most surprising, attachment of the probe did not result in any significant changes in the rotational mobility of the probe as compared to free pyrene. These results convincingly demonstrated that both bound and dispersed probes reported from similar locations within the material, showing that dispersed probes associate with the pore wall (once sufficient solvent is removed from the matrix), and thus report predominantly on the properties of the nanocomposite material itself.

More recent studies have been conducted to compare the environment and dynamics of a dansyl chromophore that was dispersed or attached to a silica matrix.[48] Using time-resolved intensity decay measurements analyzed via a distributed fitting model, it was determined that the dispersed dansyl probe experienced an environment that was more dipolar, more dynamic, and more homogeneous relative to the environment experienced by the bound dansyl probe, in contrast to the earlier study with pyrene.[47] A model to describe this phenomena was proposed and envisioned that the dispersed dansyl probe was located at or near the pore surface, but associated primarily with silanol groups at the surface. Covalently bound dansyl, on the other hand, was assumed to be distributed between SiO_2 and SiOH rich regions, with the SiO_2 region being more rigid and heterogeneous than the SiOH region. Partitioning of the probe into the SiO_2 region was speculated to be due to the hydrophobic tether linking the dansyl to the glass. Overall, these two studies clearly demonstrate that subtle changes in the nature of the probe can lead to the probe reporting from a different region within the nanocomposite; thus, it is important to determine exactly how the probe may interact with the different regions of the material.

Summary of Class II Materials. The addition of a covalently anchored dopant into silica-based materials provides a wide range of control over the polarity of the final materials. Low levels of organosilanes tend to disperse well within the material and tend to reside at the solvent−silica interface, thereby reducing the number of silanol groups (and the amount of bound water) and providing gradual changes in the final polarity of the material. The addition of higher levels of organosilanes (25 mol % or more) can lead to phase separation, perhaps owing to the existence of a critical point for self-association of the organic components, but it appears that increasing the organosilane level further (50% or higher) results in more homogeneous materials again being produced. A key problem with organosilane dopants is the lower degree of cross-linking within the final material, which can lead to poor mechanical stability. On the other hand, this same effect appears to increase the pore size and may play a role in improving the mobility of species in the glass, owing to coating of the charged silica surface. Hence, careful

Table 4. Typical Dopants Used To Form Class I Nanocomposite Materials That Have Been Studied Using Fluorescence Methods

dopant	refs
poly(vinyl alcohol)	55, 56
poly(ethylene glycol)	32, 53, 54, 55
poly(methyl methacrylate)	49, 61
poly(vinyl alcohol) graft 4-vinyl pyridine	59
poly(tetrahydrofuran)	50
poly(ethylene oxide)	60
poly(propylene oxide)	60
poly(dimethysiloxane)	51
dextran	59
nafion	32, 63, 64, 65
ionene 6,2	32
triton X-100	32,61
CO-520	61
hydroxyethyl methacrylate	61, 62
polyoxyethylene nonylphenyl ether	62
sodium dodecyl sulfate	73, 74
cetyltrimethylammoniumbromide (CTAB)	69, 70, 71, 76
poly(diallyldimethylammonium chloride)	69
phospholipids	78, 79
yeast cells	75

control over the levels and types of organosilanes is needed to simultaneously impart useful polarity, structural, and dynamic properties to the material.

B. Materials with Dispersed Organic Additives (Class I Materials). The development of class I materials generally involves the dispersion of hydrophobic, hydrophilic, or charged polymers or surfactants into TEOS- or TMOS-derived silicates during the hydrolysis step, as summarized in Table 4. Such materials can either interact with the silica, thus modifying the properties of the solvent−silica interface, or can segregate into independent phases, resulting in unique structures such as interpenetrating polymer networks (IPNs). In this section, we describe how fluorescence methods can be used to provide insight into the polarity, mobility, and heterogeneity of the final material and how such parameters are influenced by the type and level of additive. It must be noted that the materials described in this section are formed with low levels of dopants, such that self-assembled structures (and hence mesostructured materials) are not produced. Templated materials are considered in the section following this one.

Hydrophobic Polymer Dopants. Very few studies exist detailing the use of fluorescence to study hydrophobic polymer materials doped in silicate glasses. This is likely due to the poor solubility of such species in the silica sol, which is a mixed alcohol:aqueous phase. However, the limited studies on such systems have revealed some interesting results. For example, Bright and co-workers[49] have used PRODAN to probe the microenvironment of silicate materials impregnated with poly(methyl methacrylate) (PMMA), which is a relatively hydrophobic polymer that is not soluble in water. Using shifts in the emission maximum of PRODAN, it was determined that the probe was experiencing a nonpolar environment in the composite material, consistent with partitioning of the hydrophobic probe into a PMMA-rich environment. The presence of distinct subphases within the material was consistent with the formation of an interpenetrating polymer network, with the PMMA intertwining through the silica colloids, as shown in Figure 4.

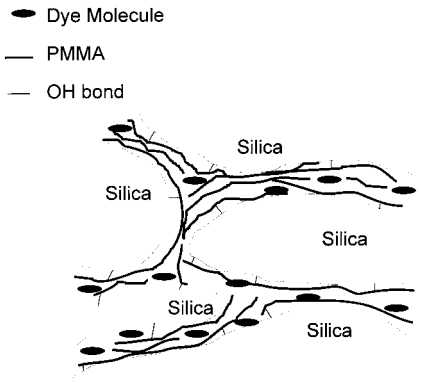

Figure 4. Structure of a PMMA−silica interpenetrating polymer network, showing the PMMA (black lines) intertwining through the silica network. The dye is shown associating predominantly with the hydrophobic polymer phase. The thin lines represent OH groups on the silica surface that interact with the polymer (adapted from ref 49).

The formation of distinct subphases within polymer-doped sol−gel-derived matrixes has also been demonstrated by Ilharco and Martinho using 1,12-bis(1-pyrenyl)dodecane as a probe in TEOS-derived glasses doped with low-molecular weight (MW 2000) polytetrahydrofuran (PTHF).[50] This probe is able to form an intermolecular excimer (via stacking of the two pyrene moieties), but the ability to form the excimer is dependent on the local polarity and conformational flexibility of the probe when present in the nanocomposite material. Emission spectra consistent with the pyrene monomer are obtained from this probe when it is in its extended form in nonpolar solvents. However, in cases where the alkyl chain interacts with polar environments, the chain collapses on itself, placing the two ends of the polymer in close proximity and producing pyrene excimer emission, as shown in Figure 5. When present in neat TEOS-derived materials, the probe exhibited a large excimer emission band, consistent with the probe interacting with the silica surface and cyclizing to minimize exposure to the polar interface. Addition of PTHF to the matrix produced a 2-fold reduction in excimer emission relative to the monomer emission intensity, consistent with the probe associating with the hydrophobic polymer and thus adopting a more extended conformation. However, the emission lifetime of the probe was multiexponential, consistent with partitioning of the probe between both environments. This suggested that the probe was distributed between the silica and the polymer phases or may have existed at the interface between the organic and inorganic phases. It was also determined that the presence of the polymer enhanced the overall dynamics of the probe, owing to the more dynamic motion of the organic polymer relative to silica, and improved the accessibility of the probe to oxygen, consistent with a more open structure in the material and preferential partitioning of O_2 into the hydrophobic phase.

A more detailed study of the environment and dynamics of polymers within sol−gel-derived nanocomposite glasses used a dansyl-labeled poly(dimethylsiloxane) (PDMS) incorporated into TEOS to produce an IPN.[51] The authors employed red-edge excitation methods to probe the environment of the probe and how it was affected by the rigidity of the local environment.

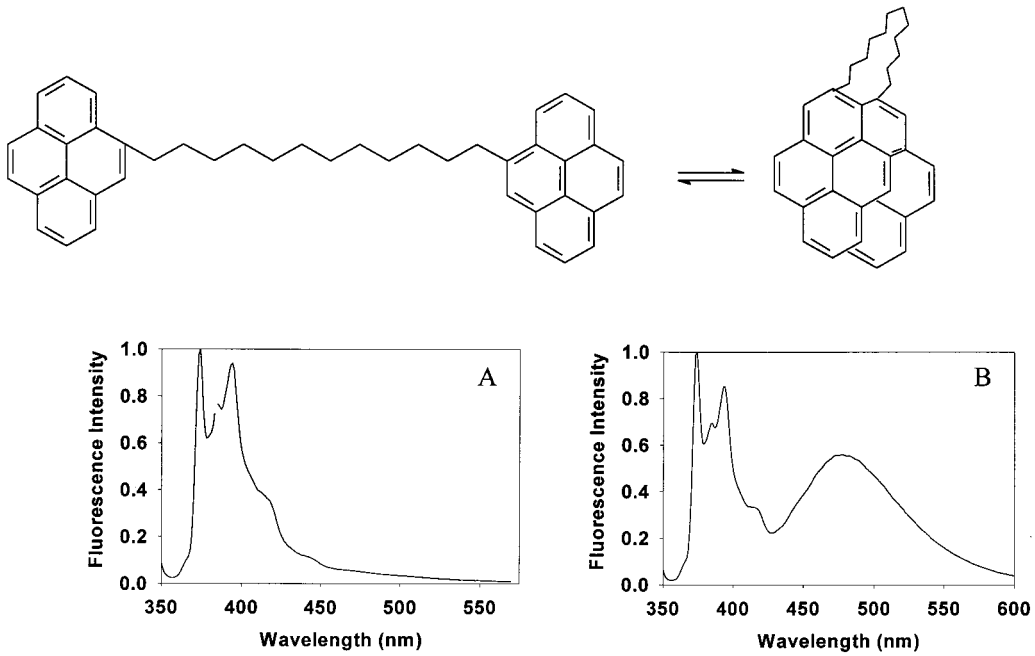

Figure 5. Open and closed forms of 1,12(bispyrenyl)dodecane and the corresponding emission profiles of (A) the extended form (monomer emission) and (B) the compact form (excimer emission) (adapted from ref 14).

In the dansyl probe, rotation of the dimethylamino group relative to the naphthalene ring results in emission from a low-energy charge-transfer state.[52] In rigid media, this rearrangement is restricted, and hence the probe relaxes from a higher energy state. Hence, a higher energy emission maxima is obtained with higher excitation energies as the rigidity of the environment increases.

PDMS−TEOS composites were prepared by precipitating the silica around the polymer using different acidic or basic catalysts. Fluorescence spectra from all samples showed inhomogeneous broadening, indicative of a distribution of environments. This was suggested to be due to a variation in the rigidity of the cages around the polymer. Using basic hydrolysis, the emission was consistent with colloids of silica surrounded by the polymer, whereas acidic hydrolysis resulted in silica fibrils, which formed an IPN that was more amenable to swelling and hence was less rigid. The rigidity of the environment of the dansyl, as revealed by red-edge excitation studies, was low for the dansyl bound to the polymer in the absence of the silica (no red-edge effect, therefore highly mobile). However, dansyl−PDMS within composites formed from ethylamine, acetic acid, or formic acid showed significant red-edge effects. These studies showed that relaxation of the excited state was substantially restricted in the composite materials, suggesting that the silica acted as a reinforcing component in the PDMS materials.

Overall, these studies suggest that hydrophobic polymers tend to form unique phases within silica-derived nanocomposites (as expected given the high polarity of TEOS/TMOS-derived materials) and that the probe generally associates preferentially with the polymer phase, which is consistent with expectations for a hydrophobic probe. Hence, the overall environment within the material is expected to be very polymer-like, but is perturbed by the presence of the silica, such that the local environment surrounding the probe is significantly rigidified, leading to lower mobility for the entrapped probes.

Hydrophilic Polymers. The incorporation of hydrophilic polymers within silicate materials is substantially more common, owing to their miscibility with the silica sol, and thus a number of fluorescence studies have been done on such polymer−silica nanocomposites. Perhaps the most common additive used to dope silicate materials is poly(ethylene glycol) (PEG), which has been dispersed into silica at various levels and molecular weights and examined using a variety of probes. PEG is relatively polar and thus is expected to associate strongly with the solvent−silica interface. However, the segregation of PEG into unique phases is also possible, and thus it is important to examine the microenvironments within PEG-doped nanocomposites at the molecular level to gain insights into how the concentration and molecular weight of PEG additives alters the properties of the material.

A number of studies have focused on the differences between high and low molecular weight PEG dopants in TEOS-derived materials. For example, Bright and coworkers have used fluorescence methods to examine materials in which up to 5% (v/v) of PEG 200, 300, or 400 was added to TEOS-derived materials.[32] The polarity of the internal environment was assessed using the pyrene I_1/I_3 emission ratio and showed that the pyrene probe experienced microenvironments that were less polar than those that had been detected in the undoped materials. However, in contrast, the same group has also reported that the inclusion of 5% PEG 8000 into TMOS-derived glasses increased the polarity experienced by pyrene relative to that of the undoped glass.[53] It was also noted that the changes in polarity saturated at a relatively low level of PEG 8000 (3% m/v) and that this additive led to decreased surface areas for the pores and lower accessibility of pyrene to O_2. Together, these results suggested that PEG 8000 segregated into a unique PEG-rich phase which preferentially interacted

with and sequestered the pyrene probe, while the lower molecular weight PEG remained dispersed in the silicate material and therefore did not form a unique phase. Such a possibility is in agreement with studies by Lesot et al.,[54] who used NMR, EPR, and DSC to study silicate samples containing high molecular weight PEG at levels up to 50 mol %. These studies indicated the existence of a biphasic system in which the PEG phase wrapped around the silica aggregates. This effect likely limited the range over which the high molecular weight PEG was able to influence the internal polarity within the composite, as the polarity experienced by the probe was effectively identical to that of the probe in neat PEG.

To further explore the question of how PEG alters the microenvironment in Class I nanocomposites, Keeling-Tucker et al. investigated the emission of 7AI and PRODAN in tetraethyl orthosilicate monoliths containing relatively low levels of PEG 400 and PEG 600.[55] When incorporated into TEOS-derived materials, both probes displayed PEG-dependent emission spectra that evolved as the internal water was expelled. Both 7AI and PRODAN indicated that the inclusion of PEG produced a very nonpolar final environment, consistent with the results obtained by Bright and co-workers for pyrene-doped materials.[32] The lack of a 420-nm peak for PEG-doped samples containing 7AI was particularly important, as this result revealed that the PEG dopant interacted with the silanol groups at the silica−solvent interface, blocking interactions between 7AI and the silica surface. This possibility is consistent with the lower surface areas reported by Bright for silicates doped with PEG 200−400.[32]

Emission spectra from entrapped PRODAN also revealed significant changes in the material properties for PEG-doped samples as compared to those for pure silica. Specifically, the peak at 430 nm (assigned to PRODAN aggregates) grew in intensity as undoped materials aged, but was not present for samples containing PEG. Thus, inclusion of the polymer caused solubilization of the probe and eliminated aggregation, as was observed for organosilane-doped materials. PRODAN emission spectra also revealed that washing the material immediately after gelation caused a substantial portion of the PEG to be removed, producing emission properties similar to those obtained in pure silica. This result affirmed that the lower molecular weight PEG dopants were freely dispersed within the material rather than intercalated within the siloxane network.

The mobility of dopants and external reagents within PEG-doped samples has also been examined for materials containing both high and low molecular weight polymers. The reorientation time of R6G in materials doped with PEG 8000 revealed two discrete microdomains,[53] in agreement with previous studies of pure TEOS-derived materials.[27a] The faster rotational component was ascribed to a primarily fluid environment (the pore solvent) while the slower reorientation time was assigned to a more viscous PEG-loaded region. Interestingly, the R6G was found to be more mobile in the PEG-doped composites formed from PEG 8000, but somewhat less mobile in samples containing PEG 200−400. In the latter case, the presence of the polymer reduced the dynamics of the probe by 5-fold compared to that of the pure TEOS glass and 10−15-fold compared to that of the pure dopant itself. These results demonstrated that the higher molecular weight PEG likely phase-separated, producing a polymer-rich phase in which probe mobility was enhanced (more like the probe in the neat polymer), while the low molecular weight material adsorbed to the pore walls, resulting in blockage of the pores and thus restricting mobility.

Another additive that has been widely used to modulate the internal environment of sol−gel-derived glasses is poly(vinyl alcohol) (PVA). This dopant has been utilized extensively in sol−gel-derived materials, primarily as a stabilizer of entrapped proteins such as lipase,[56] acetylcholinesterase,[57] and glucose oxidase.[58] Although this additive has been widely employed in sol−gel glasses, surprisingly few reports exist on fluorescence studies of PVA-doped silicates. A recent study[55] used 7AI and PRODAN to probe glasses doped with PVA (MW 13 000) and has shown that addition of this polymer produces a very hydrophilic environment, consistent with association of the probes with the hydrophilic polymer. Addition of the polymer to the TEOS-derived materials also resulted in a substantial increase in optical scattering, suggesting that the polymer segregated into a unique phase. The scattering may have been the result of precipitation of the polymer within the glass (PVA-13000 is a solid at room temperature), further supporting segregation of the PVA into a unique phase.

Another hydrophilic polymer that has been examined in silica glasses is dextran (MW 70 000), which was labeled with the pH-dependent probe fluorescein along the polymer backbone to allow polymer dynamics within the silicate materials to be assessed.[59] Two main conclusions were drawn from the study. First, the probe pK_a was higher in the glass, which is in keeping with previous observations that the pH inside the glass is lower than that in bulk solution, owing to the negative charge on the silicate surface.[14] Second, it was determined that the polymer was only slightly less mobile in glass than in solution, indicating that the entrapped polymer retained significant conformational freedom, indicative of minimal polymer−silica interactions. The enhanced mobility was attributed to macroscopic phase segregation, wherein the polymer existed in a phase that was primarily polymer-rich (and thus similar to solution), while the silica formed a unique polymer-depleted phase, consistent with the results obtained from high molecular weight PEG and PVA.

Recent studies of polymer-doped silicates have examined the effects of covalently anchoring a fluorescently labeled polymer to the silica, producing a Class II material that mimics a polymer-dispersed class I material. Stathatos et al. conducted a time-resolved fluorescence study of thin films composed of silica grafted with poly(ethylene oxide) (PEO) or poly(propylene oxide) (PPO).[60] By monitoring the I_1/I_3 ratio for entrapped pyrene, it was found that the internal polarity was intermediate between the polymer and silica phases, suggesting that the probe may have existed at the interface between these phases. Excimer formation was also enhanced in the PEO- and PPO-doped samples, suggesting that the polymer component was able to organize by hydrophobic interactions to provide a rela-

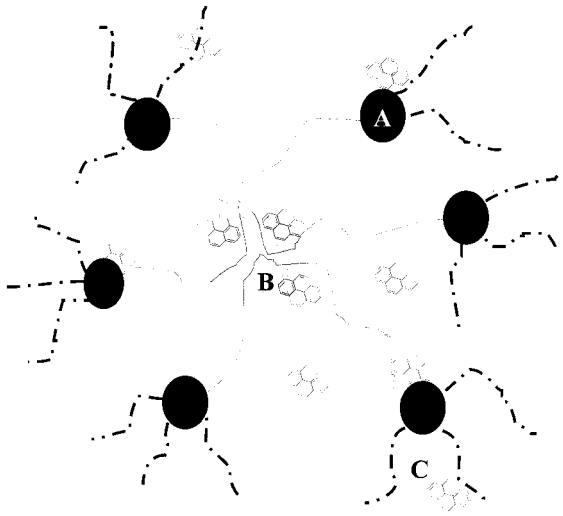

Figure 6. Organization of nanocomposites into two mesoscopic domains containing inhomogeneously dispersed fluorescent probes. Situation (A) shows probe molecules that are associated with the silica colloids, situation (B) shows probes associated with the polymer phase, and situation (C) shows the probe that is in a solvent phase, as observed at early aging times (adapted from ref 60)

tively large volume fraction of the organic subphase. On the other hand, composite materials containing short PEO or PPO chains were similar to pure silica in terms of polarity, consistent with the probe associating predominantly with the silica surface. Hence, the longer polymer chains likely resulted in separate inorganic and organic phases within the material, while the shorter chains dispersed throughout the material, producing a smaller overall effect on material properties.

Energy transfer between pyrene and coumarin-153 was also examined for these polymer:silica composites[60] and was analyzed using stretched exponentials to determine the dimensionality of the donor−acceptor distribution. Stretched exponential analysis is useful in cases where the probe quenching occurs in restricted geometries. In such a case, the number of sites that a quencher visits within a time interval t is defined by a random-walk process and is proportional to t^f ($0 < f < 1$). More restricted environments lead to time-dependent quenching rate constants because quenching efficiency will depend on the distance between the quencher and probe at the time of excitation and thus on the rate of diffusion within the glass. This is manifested as a lower value for f.[16] With smaller polymer chains it was found that there existed a very restricted environment for both probe molecules (small f value). In contrast, larger chains showed a much higher f value, presumably because of a larger organic domain that was extensive enough to allow molecular diffusion, in agreement with SAXS studies on similar systems.[12] The two-state model developed from these studies is represented in Figure 6 and shows silica colloids dispersed in a polymer phase, with the pyrene probe partitioning between the organic and inorganic phases. This model suggests that, for very high molecular weight polymers, the organic polymer dominates the material behavior, while the silica acts as a secondary component, in agreement with studies of PDMS−silica composites.[51]

Surfactants and Charged Additives. The production of Class I materials has also made use of other low molecular weight surfactants and charged additives dispersed in the inorganic material. Such dopants include Triton X-100 (a nonionic, amphiphilic surfactant), Nafion (a perfluorosulfonic acid ion exchanger), and Ionene 6,2 (a linear diammonium ionomer).[32] Inclusion of such dopants at low levels (well below the critical micelle concentration, CMC) results in dispersion of the dopants within the glass and generally does not result in self-assembled structures or mesostructured materials. The dispersion of low levels of surfactants within silica was confirmed using pyrene emission, which indicated that incorporation of these additives led to only very small changes in the polarity of the composite, as compared to undoped TEOS (pyrene would be expected to partition into a micellar structure and thus would report a very nonpolar environment if micellar structures existed). Steady-state anisotropy measurements of R6G suggested that the probes were somewhat more mobile at low dopant levels (as compared to pure silica), but often became restricted in mobility when higher dopant levels were employed, generally returning to the levels observed in pore TEOS-derived materials. Overall, the results suggested that low levels of amphiphilic dopants did not alter the internal environment significantly, at least from the perspective of pyrene and R6G.

To further assess the effects of amphiphilic dopants on the behavior of sol−gel-derived silica, Del Monte and Levy[61] examined the emission of the probe 1,1′3,3,3′,3′-hexamethylindotricarbocyanine iodide (HITC) in nanocomposites composed of TMOS and either Triton X-100, CO-520 (a neutral surfactant), PMMA, or hydroxyethyl methacrylate (HEMA). In all cases the dye showed a longer lifetime in the doped glasses than in neat TMOS-derived samples, which was taken to be an indication of higher rigidity arising in the presence of the dopant. This was assumed to be due to a covering of the pore walls with the dopants, leading to adsorption of the amphiphiles and their associated probes onto the silica surface, producing a restriction in probe motion.

Later work by Levy and co-workers[62] used the probe oxazine-1 to examine the polarity and mobility of films containing low levels of dispersed nonionic surfactants such as polyoxyethylene nonylphenyl ethers (POE) and hydroxyethyl and lauryl methacrylates. In general, it was observed that the lifetime of the probe increased with increased POE chain length, with insignificant changes in wavelength. The enhanced lifetimes were ascribed to higher microviscosity values when the longer chain polymers were used, consistent with increased association of the polar headgroup of POE with the silica and, thus lower mobility. Time-resolved anisotropy decays were also obtained for oxazine-1 in these materials and were best fit to a hindered rotor model, wherein the probe was only partially free to rotate. This behavior is commonly manifested as a non-zero post-decay baseline for anisotropy decays ($r_\infty > 0$). On the basis of the values of r_∞, it was possible to obtain information on the degree of "wobble" motion for the hindered probe. For HEMA, which can re-esterify the silanols, r_∞ was high; thus, the probe was very restricted. All other polymers showed lower r_∞ values, consistent with a higher degree of motion. Viscosity values obtained from the anisotropy measurements showed that the incorpo-

ration of polymers resulted in a higher viscosity in the region of the probe, indicating that the probe was associated with the polymer phase close to the silica surface. The authors proposed a surface coated with polymer as the most likely model to describe this situation.

Further studies of the charged polymer Nafion in sol−gel-derived silica have also been done using both pyrene[63] and other probes.[64,65] Pyrene fluorescence demonstrated that the overall polarity of the matrix was determined primarily by the silane component (organosilane additives resulted in lower polarity), with only a very small effect from the charged polymer. This is consistent with the hydrophobic probe being unable to associate with the charged polymer, and thus reporting from the silica phase. Higher levels of Nafion caused the SO_3^- groups to be in the vicinity of the probe, thus increasing the polarity, likely owing to high levels of associated waters of hydration. This was confirmed by the ability of the Nafion/silica matrix to take up water, with this ability being greater than that of Nafion alone. These results indicated that water adsorbed to both the polymer and the silica, resulting in a relatively polar microenvironment within the glass. This result suggested that such composites may be useful for entrapping samples, such as proteins or cells, that require an aqueous-like environment for optimal performance.

Summary of Class I Materials. Overall, the data from the fluorescence studies of polymer-doped silica suggest that the addition of a low molecular weight polymer results in dispersion of the polymer within the material, leading to gradual changes in polarity (the direction of which depend on the polarity of the polymer) and somewhat lower mobility, owing to blockage of the pore. Higher molecular weight polymers tend to segregate into separate phases, and the hydrophobic probes tend to associate with the polymer, resulting in significant alterations in polarity and enhanced probe mobility as compared to the more rigid silica phase. Hydrophobic polymers generally result in phase segregation regardless of molecular weight, with probes preferentially partitioning into the organic phase. This leads to enhanced diffusion and accessibility of probes and quenchers, similar to the levels observed in the neat polymer solutions. Thus, by selecting polymers of the proper polarity and size, one can tune the polarity, homogeneity, and dynamics of the nanocomposites over a broad range, with the main limitation being determined by the polarity and viscosity of the polymer itself. However, in many cases, and particularly for hydrophobic polymers, there exists a limited range over which the polymers can be incorporated, as extensive phase segregation often leads to undesirable material properties, including poor mechanical stability and low transparency, potentially limiting their usefulness in photonic and sensing applications.

6. Fluorescence Studies on Emerging Materials

A. Templated Materials. In addition to the nontemplated Class I materials described above, a number of studies have recently appeared describing fluorescence probing of templated class I materials. Most molecular templating studies aim to develop sol−gel-derived nanocomposites and films with controlled morphologies, using either surfactant-induced[66] or nonsurfactant-induced[67] templating methods. Several recent reviews highlight the many approaches used to prepare templated materials.[68] In general, templates either modify silica networks, producing ordered mesostructures such as lamellae, hexagonal arrays, or cubic phases (among others), or participate in network formation (via covalent attachment to the network), thus becoming incorporated into the silica phase. Alternatively, biological species (lipids, cells, and proteins) can be dispersed in the matrix and at appropriate concentrations will undergo self-assembly to form supramolecular structures that result in controlled alterations in the texture of the material.

Templated materials have several potential advantages over the more conventional Class I and Class II nanocomposites. As described in detail below, templating can be used to disperse supramolecular organic assemblies into a silicate matrix, which can either be retained to impart catalysis or sensing functions or removed by calcination to produce a well-ordered array of pores (leading to highly accessible materials). Furthermore, as shown below, hexagonal arrays of wells can be formed via self-assembly of cells, thus leading to the ability to produce spatially addressable sites in the material, which are potentially useful for multianalyte biosensors or HTS applications. Finally, templating approaches can be used to provide control over the location of a given species (such as a fluorophore), providing opportunities for optimization of photonic devices based on sol−gel-derived nanocomposites.

The most common method used to produce mesostructured materials is the inclusion of self-assembled structures, such as micelles, into the sol before formation of a bulk material or thin film. The micelles are typically derived from ionic surfactant molecules such as cetyl trimethylammonium bromide (CTAB) or sodium dodecyl sulfate (SDS).[66] Bekiari et al.[69,70] compared the effects of neutral and charged dopants on the transparency and internal environment of silicate glasses. Transparent materials were obtained using low molecular weight PEG (MW < 1000) or cationic surfactants such as CTAB. However, anionic surfactants produced translucent or opaque glasses, as did high molecular weight neutral surfactants such as Triton X-100. Pyrene excimer formation and energy transfer from pyrene to coumarin 153 were measured and analyzed using a stretched exponential model to further characterize the polarity and phase segregation behavior in the composite glasses. Both excimer formation and energy transfer were enhanced in the composite glasses relative to those formed from neat TMOS, indicative of higher diffusional mobility for these hydrophobic probes. On the other hand, the kinetics of the quenching reaction between the hydrophilic probes $Ru(bpy)_2^{2+}$ and methyl viologen (MV^{2+}) indicated a restriction in mobility for these species. These results were interpreted in terms of segregation of the hydrophobic probes into a micellar phase, producing significant mobility, while the charged probes were excluded and thus interacted with the more rigid silica, becoming less mobile.

The groups of Dunn and Zink have also been active in the development of a number of unique templated nanocomposites based on sol−gel-derived silica−sur-

factant hybrid films, and have used fluorescence spectroscopy extensively to characterize these materials. It must be noted that many of the common methods for investigating bulk materials, such as NMR and N_2 adsorption analysis, are not sufficiently sensitive to analyze thin films. However, the excellent signal-to-noise ratios for fluorescence measurements makes examination of ultrathin films relatively straightforward, making fluorescence spectroscopy a powerful tool for characterization of such systems.

Early work by Zink et al. aimed to determine how film evolution controlled the development of the mesostructured materials. In this work, surfactant templated mesoporous materials were formed using CTAB that was dispersed in TMOS at a concentration just below the CMC.[71] These materials were observed to form mesophases with hexagonally packed one-dimensional channels present at the solid−liquid and/or liquid−vapor interfaces. It was shown that rapid dip casting of films could result in rapid synthesis of continuous mesoporous films, showing liquid-crystalline order between the surfactant and silica phases. Furthermore, the thin films produced unique structures that were not obtained with bulk materials because the rate of solvent loss from the film was significantly more rapid than that from a bulk glass (≈12−15 s, based on the emission of pyranine[72]). As a result, the loss of solvent was generally complete before the matrix began to undergo aging, unlike the case of bulk materials where both processes occur simultaneously over a period of months.

On the basis of XRD data, it was also determined that adjusting the level of the surfactant could result in films with hexagonal, lamellar, or cubic phases. In the latter case, the pores were connected in three dimensions, which guaranteed accessibility from the surface. The mobility of dopants within these films was characterized by measuring the fluorescence depolarization of 2-*p*-toluidinyl naphthalene-6-sulfonate (2,6-TNS) to monitor the evolution of mesophases in situ. Spatially resolved fluorescence probing was done as a function of distance of the film from the reservoir and, thus, time after casting. Close to the casting well, the initial film thickness was on the order of 4 μm, as determined by IR interferometry, and was rich in ethanol. However, as the film was pulled further from the well, the thickness of the film decreased to a final value of about 350 nm and the mobility of the probe decreased sharply, owing to incorporation of the probe into the micellar phase. The formation of micelles was expected because a substantial amount of ethanol was removed from the film at the initial stages of drying, causing the surfactant to exceed its solubility in the water-enriched solvent. As the film was pulled further from the reservoir, the water also evaporated and the polarization of the probe continued to increase significantly, consistent with incorporation of the probe into the micellar phase. Without CTAB present, the polarization began to increase only above the drying line, owing to adsorption of the probe onto the silica.

Later work by Zink and co-workers has extended the initial work with CTAB−silica nanocomposites to a variety of other templating agents, including SDS, polymers, and even whole cells. Studies on SDS−TEOS nanocomposites showed that lamellar films with alternating surfactant and silica layers were produced upon dip casting of SDS−TEOS mixtures.[73] In this work, pyrene was used to assess micelle formation, while solvent composition was assessed using pyranine. Pyranine fluorescence indicated that the maximum level of entrapped water during dip casting of the film was higher than that for pure silica films (60% vs 40%), suggesting that the ionic surfactant aided in retaining water within the film. In contrast to the materials formed from CTAB,[71] pyrene I_1/I_3 emission ratios for the SDS−silica materials showed that the micelles formed at early times (as for the CTAB−silica system) but then underwent a reorganization owing to a phase transition, producing both a higher polarity and higher mobility for the probe, consistent with exposure of pyrene to the aqueous phase. Finally, as film formation neared completion, the pyrene emission again reflected a nonpolar and highly immobile film structure, consistent with reformation of ordered lamellar structures and incorporation of the hydrophobic probe into the organic phase. The entire formation−reorganization−reformation process occurred over a total time of only 12 s, as the solvent was lost from the film during casting. This clearly demonstrates that the films are very dynamic in nature during the casting process and suggests that careful control over casting speed, solvent composition, and surfactant concentration is important when attempting to form mesostructured materials.

Examination of the excimer emission from pyrene in the SDS−silica nanocomposite was continued over several weeks and showed that the films continued to re-organize over 10−15 min to produce a more stable structure, which then slowly evolved to a final structure over a period of several weeks.[74] Thus, even though the initial evolution of the film was very rapid (10−15 s), owing to solvent loss, the aging processes (continued condensation and syneresis) continued for many weeks before a stable film was obtained. It is also interesting to note that even after weeks of aging the pyrene was still able to form an excimer, indicating that the flexible hydrophobic tails of the surfactant allowed for at least some degree of local mobility. This suggested that even though the rotational mobility of pyrene was restricted (as determined by rotational anisotropy measurements), translational motion of the probe along the planes of the surfactant tails was still possible, and hence complete loss of probe mobility was not observed. Thus, it is possible that such materials may be able to provide a degree of conformational motion to entrapped probes, which may be important for development of photochromic devices.

More recently, Zink and co-workers used yeast cells as templates to prepare mesostructured silica materials.[75] Here, the spherical yeast cells packed into a hexagonal array in the thin silica film, leading to the potential for spatially addressable cell-based biosensors. The fluorescent dye 2,6-diamidino-2-phenylindole (DAPI) was able to stain the intracellular DNA, proving that the cells were accessible to external reagents even when entrapped. Such systems could prove to be very useful for spatially addressable sensors or drug-screening chips, particularly if the cells are engineered to have reporter genes that encode green fluorescent protein, thus resulting in a multichannel fluorescence sensor.

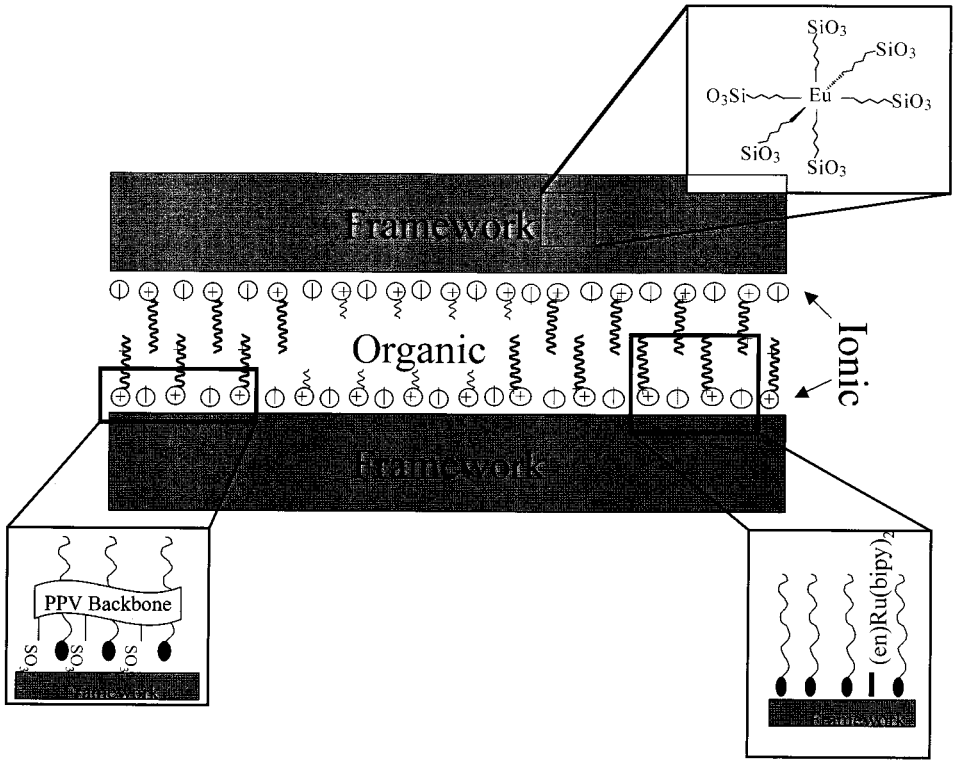

Figure 7. Schematic representation of the location of fluorescent probes within mesostructured sol−gel films. The framework consists of silica, while the organic region contains the hydrocarbon tails of the surfactant templates, and the ionic region contains the surfactant headgroups and counterions (adapted from ref 76).

A key problem with many nanocomposites is the inability to control the location of the fluorescent probe within the matrix. In fact, as discussed above for both class I and class II nanocomposites, the probes are typically dispersed in the sol, and thus their final location is determined solely by the solubility of the probe in either the organic or the inorganic phase. Zink and co-workers have addressed this problem by using molecular templating to control the location of the fluorophore within the surfactant−silica nanocomposite.[76] Three approaches were utilized. In the first, Eu(III) was bound to three *N*,*N*-bis(triethoxysilanepropyl)-2,6-pyridine dicarboximide ligands in the presence of CTAB as a template and entrapped in a TEOS-based glass. Luminescence measurements of Eu(III) indicated that the ion was bound to the silica portion of the nanocomposite, as desired. In the second approach, a fluorophore-tagged ionic polymer, (2,5-methoxypropyloxysulfonate)phenylene vinylene), was added to a CTAB−silica nanocomposite that formed a hexagonal-phase mesostructured material. Here, the organic backbone of the polymer was incorporated into the organic region of the film, while the sulfonate groups interacted with the ionic interface region, as depicted in Figure 7. Fluorescence polarization measurements indicated that the labeled polymer was preferentially aligned in the mesostructured film such that the polymer was oriented along the rods of the hexagonal structure, within the cylindrical micelles. The final method used to control the location of the fluorescent probe utilized a silylated Ru(II)bipyridine complex that was covalently attached to the silica. In this case, the charged probe was preferential loading at the interface between the organic and inorganic regions, where the charged headgroups of the CTAB were located. This work clearly shows the ability to control the placement of fluorescent molecules within nanocomposite materials and represents a significant advancement, as it may open up routes to new photoactive materials with the photoresponsive molecules placed carefully into regions of high mobility (which is needed for photoswitchable species) or low accessibility to O_2 (to reduce photo-oxidation and improve probe stability).

Molecular imprinting of fluorescent species has also been used to form templated materials that were appropriate for selective sensing of polyaromatic hydrocarbons. In work by Katz and Davis,[77] sol−gel silica was imprinted with single aromatic rings carrying one, two, or three APTES side groups (initially protected as carbamates to avoid side reactions). The amino end of the APTES was bound to the aromatic ring, while the triethoxysilane terminus allowed covalent attachment of the APTES to the silica, thus generating microporous media with functional organic groups. Residual silanol groups were then capped with TMS chloride or 1,1,1,3,3,3-hexamethyldisilazane, and the aromatic core was removed via reaction with trimethylsilyliodide to creat a cavity with spatially organized amino groups on the pore wall, producing a shape-selective cavity. The ability of the materials to selectively bind aromatic species was tested by introducing pyrenebutyric acid (PBA) into one- and three-point materials (i.e., samples containing one APTES per pore or three APTES spatially arranged in a single pore). Pyrene emission spectra indicated that one-point materials produced monomer emission, while the three-point material resulted in excimer emission. This result indicated that one-point materials result in site isolation of individual probes (as expected because there was only one site for interaction of the butyric acid group with the amine), while three-point materials could

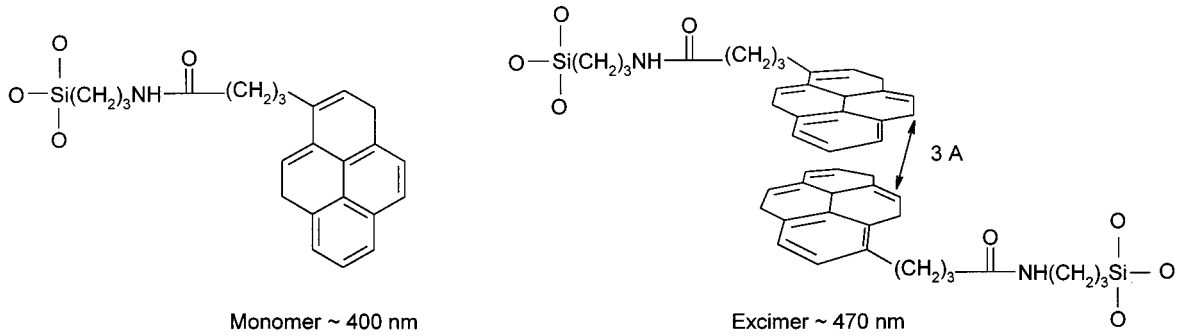

Figure 8. Schematic of pyrene bound into molecularly imprinted silica materials. (A) Binding by one-point materials results in site isolation of individual probes, producing monomer emission. (B) Binding by three-point materials leads to pyrene clustering, resulting in excimer formation. (For clarity only two of the three pyrenes are shown.) (Adapted from ref 77.)

bind up to three pyrene molecules, leading to clustering of the probe due to closer contact of the pyrene moieties in cavities with three amines, as illustrated in Figure 8.

Summary of Templated Materials. The examples cited above clearly demonstrate that incorporation of supramolecular assemblies into sol−gel-derived silica can lead to a number of unique mesostructured materials. Furthermore, it is clear that by carefully selecting both the templating species and the probes, one can control the final location of the probe (i.e., the polar silica surface, the nonpolar surfactant phase, or the interfacial region between these phases). The ability to probe mesostructured films in real time and in situ by fluorescence spectroscopy has clearly shown that mesostructured films undergo substantial changes at the molecular level for many weeks, even though macroscopic measurements, such as XRD, show no changes in the material structure. Furthermore, fluorescence measurements reveal that the surfactant phases within such materials retain significant mobility, which is potentially beneficial for the development of photochromic or sensor devices. Finally, the ability to spatially control the location of pores within such materials using molecular templates is likely to have far-reaching ramifications because it can be used to control the accessibility of entrapped probes or to produce spatially addressable sensor devices.

B. Biomaterials. *Overview.* A final type of class I material that has been extensively studied by fluorescence methods is biomolecule−silica nanocomposite biomaterials. These materials are typically composed of either liposomes (as mimics of whole cells) or proteins. In the case of liposomes, a key question is whether these fragile structures remain intact upon entrapment and whether they undergo normal solution-based behavior such as phase transitions and trans-membrane ion transport. Protein-based biomaterials have been widely touted as platforms for biosensor devices, affinity columns, biocatalysis systems, and drug-screening platforms and thus rely on entrapment of the biomolecule in a functional form. These biomolecules can, to a first approximation, be thought of simply as large biopolymers. However, the specific three-dimensional structures of proteins and the distribution of charged sites on the protein surface make such molecules much more challenging to entrap and can lead to unique interactions between the protein and the silica. Furthermore, subtle changes in protein conformation or dynamics can alter their ability to perform their normal biological function; thus, it is important to understand how entrapment affects proteins and how the presence of the protein in turn may alter the material properties. In this section, we consider class I materials composed of either liposome−silica or protein−silica composites and address the question of what new insights into biocomposites are made available by fluorescence studies of such materials.

Liposomes. The incorporation of lipsomes into silica provides a new type of material that has the potential to result in improved sensor or drug-delivery platforms.[78,79] In a recent report, polymerized diacetylenic liposomes (prepared as small unilamellar vesicles, average diameter 50 nm) containing 5 mol % of a pyrene-labeled lipid were entrapped into TMOS-derived silicates to develop a sensor for heavy metals and viruses.[78] The pyrene emission was consistent with the entrapment of intact vesicles, having an I_1/I_3 emission ratio that was indicative of a nonpolar phase. It was demonstrated that interactions with metal ions or changes of pH resulted in alterations in pyrene emission that were consistent with structural reorganization within the entrapped liposomes. This result confirmed that the liposomes remained intact and that the lipids were able to undergo sufficient local translational motion in the plane of the bilayer to allow phase transitions to occur. The sensitivity to metal ion concentration was enhanced by a factor of 50 relative to solution, suggesting that the local metal ion concentration within the glass was increased, owing to electrostatic attractions with the negative silicate. Another surprising finding was that entrapped liposomes doped with sialic acid were able to respond to intact viruses, via binding to the hemagglutinin lectin on the surface of the influenza virus, producing a purple-red color change. This result indicated that the virus could enter the glass, even though it was large (≈50−100-nm diameter) and negatively charged, while the liposomes remained entrapped. This suggested that the pores within these glasses were relatively large (≈100 nm), consistent with molecular templating, but that the liposomes remained in the material, owing to strong associations with the silica network, or templating of the silica around the liposome.

Incorporation of fluorescein-loaded liposomes into TMOS-derived materials has recently been utilized for the development of a pH sensor.[79] The liposome was used as a container to reduce leaching of the free dye from the glass and avoided the need for covalent

Table 5. Fluorescent Proteins Used for Probing Sol−Gel-Derived Materials

protein	parameter measured	information	refs
HSA	acrylodan emission wavelength	protein tertiary structure	84
	acrylodan rotational anisotropy	protein mobility	84
	acrylodan lifetime	heterogeneity of microenvironments	84
BSA	tryptophan quenching	accessibility	80, 89
	acrylodan emission wavelength	protein tertiary structure	84
	acrylodan rotational anisotropy	protein mobility	84
		effects of PEG	53
antidansyl	dansyl emission intensity	binding constant	86
antibody	dansyl rotational anisotropy	protein mobility	86
antifluorescein antibody	intensity and anisotropy	time-dependent changes in protein behavior	87
monellin	Trp emission wavelength	conformational motions	81a
	quenching	response kinetics	81a
		accessibility	81b
	Trp intensity vs temperature	protein stability	81b
		rotational mobility	81a
cod III parvalbumin	Trp intensity	Ca(II)-induced conformational changes	81d
		binding constant	81d
	quenching by acrylamide	protein conformation	81d
oncomodulin	sensitized Tb(III) luminescence	binding constant accessibility regenerability	81c
myoglobin	Trp emission intensity	conformational motion	80
	rotational anisotropy	protein mobility	85
alcohol dehydrogenase	Trp emission wavelength	protein conformation	82

conjugation of the dye to the surface of the silica. Fluorescence imaging of the glass revealed that intact spherical liposomes (70-nm diameter) were entrapped in the glass. A useful finding in this case was that the pH response of the dye was extremely rapid (<1 s) and had an identical pK_a to that in solution, indicating effective shielding of the dye from the silica surface. It was also noted that the encapsulation of the probe in liposomes eliminated leaching (as compared to free probes in glass, which showed a 60% loss in intensity over 12 h). Hence, by combining an organic and inorganic phase, improved performance was obtained for a simple sol−gel-based optical pH sensor.

Encapsulated Proteins. The incorporation of fluorescent proteins into sol−gel-derived nanocomposites provides a unique reporter of internal microenvironments in such materials. Table 5 provides a listing of the various fluorescent biomolecules that have been used to examine sol−gel-derived nanocomposites. Such species are generally added to the hydrolyzed precursors along with appropriate buffer salts to initiate gelation and thus end up dispersed within the matrix. The protein may either be intrinsically fluorescent, owing to tryptophan or flavin adenine dinucleotide (FAD) moieties, or can be labeled with an extrinsic probe, either randomly or site selectively. As described below, the study of fluorescent proteins in sol−gel-derived silicate materials can provide information on the structure, dynamics, activity, accessibility, and ligand binding constants for entrapped proteins. Because the biomolecules are large compared to small fluorescent probes, one gains insight into whether large dopants may block the pores in the glass, whether charged biological dopants may template with the silica, and whether the pores are sufficiently large to allow conformational changes for the entrapped biomolecules. These studies are briefly summarized below.

(1) Conformational Motions. Several studies on the conformational motions of entrapped proteins have made use of the intrinsic fluorescence of tryptophan.[80−82] The emission characteristics of the indole group of tryptophan are known to be highly sensitive to the polarity of the surrounding solvent, with a red-shift to longer wavelengths being common when the hydrophobic amino acid becomes exposed to solvent during the unfolding of a protein.[16] The earliest study of Trp fluorescence from an entrapped protein was by Saavedra, who examined the conformational flexibility of bovine serum albumin (BSA) and myoglobin entrapped in TMOS-derived glasses.[80] The emission of the Trp residue was consistent with the BSA remaining in a native conformation upon entrapment, although the conformational motions of the protein, as determined from pH and guanidine hydrochloride-induced conformational changes, were restricted for the protein in the glass. The emission spectrum of myoglobin, on the other hand, was red-shifted, consistent with partial unfolding of the protein upon entrapment.

Our group has also made extensive use of tryptophan fluorescence to examine the proteins within sol−gel-derived biomaterials.[33,81] Thus far, all proteins that we have studied (monellin, parvalbumin, oncomodulin, and human serum albumin) have retained nativelike emission properties, consistent with the entrapment of correctly folded proteins. This is an important finding as there is typically up to 35% (v/v) of ethanol present during protein entrapment, which has been reported to cause denaturation of some proteins during entrapment.[83] Furthermore, all proteins were able to undergo either analyte- or denaturant-induced conformational changes, consistent with the presence of large pores within the hydrated glasses. However, it was often observed that proteins were not able to fully unfold with the silica-based glasses, in agreement with the results reported by Saavedra et al.[80] This finding is consistent with partial restriction of the conformational changes, owing to protein−silica interactions. This suggests that the pores within the hydrated glass are larger than those in dried glasses (i.e., >10 nm), but are still not large enough to accommodate the fully unfolded protein (which are typically several tens of nanometers in diameter), resulting in only partial unfolding of the protein.

Entrapment of extrinsically labeled proteins has also provided some insights into the microenvironment of the protein. Bright and co-workers have examined acry-

lodan-labeled human serum albumin (HSA) and BSA entrapped in TMOS-derived glasses.[84] Time-resolved anisotropy measurements for the acrylodan probe suggested that while native protein existed immediately upon entrapment, significant structural changes occurred upon aging of the material, consistent with the formation of a more open structure for the protein, as determined by increased local motion for the acrylodan probe. Furthermore, the mean lifetime of the acrylodan probe decreased and the width of the lifetime distribution increased as the glasses aged, consistent with partial unfolding of a fraction of the entrapped protein as aging continued. These structural changes are clearly the result of changes in the internal solvent composition (owing to loss of water) and subsequent protein−silica interactions, which lead to undesirable changes in protein conformation, and suggest that measures are needed to minimize protein−silica interactions.

(2) Protein Dynamics. Measuring the mobility of entrapped biomolecules provides unique insights into the behavior of biologically doped nanocomposite materials, as it permits one to monitor the motions of a very large rotating body. Such measurements can provide insights into protein−silica interactions and internal solvent microviscosity and how these change as the material ages. The dynamics of acrylodan-labeled albumins entrapped in TMOS-derived sol−gel materials was examined[84] and showed that although the protein motion was more restricted than that in solution, the global motion of the encapsulated protein was not completely inhibited. This surprising result indicated that the protein became sequestered into pores that were both hydrated and sufficiently large to allow some degree of mobility. This is in contrast to the typical pore sizes reported for TMOS materials using BET measurements (typically <10 nm) and shows again that the hydrated glasses have substantially larger pores than do the dried materials.

While studies of BSA suggested that proteins retained global rotational motions in glass, other studies have reported contradictory results. For example, Gottfried et al.[85] measured the rotational anisotropy of entrapped magnesium protoporphyrin IX substituted myoglobin (MgMb) and detected a single rotational correlation time that was greatly increased compared to that for the protein in solution (≈1 μs vs 9.6 ns, respectively). This result indicated that the protein was essentially immobile within the glass, consistent with interactions between the matrix and the protein which would cause localization of the protein near the pore wall where global motion of the protein would be restricted.

More recently, Bright et al. showed that antidansyl antibodies were effectively immobile in glass,[86] although antifluorescein antibodies remained somewhat mobile.[87] Antibodies are typically very rigid and thus only show rotation of the whole biomolecule or some local segmental motion related to the motion of the antigen binding domain. The results suggest that the silica likely templated around the protein, leading to restricted mobility. While this is undesirable in most cases (such as for sensors or affinity chromatography), it has been demonstrated that a potential advantage of the restricted mobility is the ability to trap protein unfolding intermediates, as demonstrated by Friedman and coworkers.[88] Such trapping can allow for detailed investigations of what are normally transient species, providing unique insights into biophysical phenomena such as protein unfolding.

As is evident from the examples cited above, the vast majority of fluorescence studies involving entrapped proteins have used pure silica as the entrapment medium. However, at least one study has explored the effects of adding PEG dopants on the dynamics of entrapped proteins. In this study, acrylodan-labeled BSA was entrapped in TMOS-derived materials containing 5% of PEG 8000, and the protein mobility was compared to that obtained in pure TMOS. The results indicated that BSA was more dynamic in a composite glass as compared to a pure TMOS material, despite the higher viscosity predicted for regions containing PEG.[53] These results were interpreted as being due to preferential adsorption of the PEG to the silica surface, which resulted in enhanced mobility for the entrapped protein, owing to fewer protein−silica interactions. This result is important as it clearly shows that the microenvironment experienced by the entrapped biomolecule can be manipulated by dispersing organic polymer dopants that compete with the protein for adsorption sites on the silica surface.

(3) Accessibility of Entrapped Proteins. The examination of protein stability, reaction kinetics, and function all require that an external reagent (either a chemical denaturant or an analyte) be able to reach the entrapped protein. However, entrapment of a protein into nanometer-scale pores can result in some of the protein being entrapped in pores which are completely accessible to the analyte and some in pores that are partially accessible, while the remainder of the protein is sequestered into pores which are completely inaccessible. Hence, it becomes important to be able to determine what fraction of entrapped protein remains accessible to analytes when studying the behavior of the entrapped protein.

Proteins are particularly useful for assessing accessibility of external reagents because the inherent size-exclusion properties of the microporous glasses prevents leaching of the protein from the glass so that only analyte diffusion to the entrapped protein determines whether a reaction occurs. A particularly useful method for assessing protein accessibility is to monitor the quenching of the entrapped protein fluorescence by reagents such as O_2, acrylamide, Co^{2+}, or I^-. Accessibility studies have been done for a series of proteins entrapped in both wet-aged and dry-aged monoliths.[81e] In most cases, it has been observed that entrapment results in the presence of a fraction of inaccessible protein; however, this is highly dependent on the size of the protein. Typically, small proteins such as parvalbumin or oncomodulin (molar volume of ≈12−15 nm^3) remain completely accessible.[81c−d] Slightly larger proteins such as monellin (molar volume of 23 nm^3) show inaccessible fractions between 8% and 15%.[81b] Larger proteins such as bovine serum albumin (molar volume of 43 nm^3)[53] may have as much as 50% of the protein located in inaccessible regions of the glass, with the inaccessible fraction increasing as the materials dry.[80,89] These results suggest that larger proteins may block the entrances to the pores within which they reside, making

it impossible for analyte to enter and interact with the protein.

(4) Function of Entrapped Proteins. Perhaps the most important issue regarding entrapped proteins is whether they remain functional and to what degree. The function of an entrapped protein depends on a number of factors, including the protein location (related to accessibility of the protein, as described above), protein structure (native vs unfolded), and the charge and polarity of the local environment, which can affect the binding properties of the protein (turnover number, catalytic constant or Michaelis constant for enzymes, association, dissociation, or affinity constants for antibodies or metal-ion-binding proteins). These parameters will determine whether full or partial function remains after entrapment, how the binding characteristics of the protein change on entrapment, how the binding properties change over time, and to some extent, whether binding of analyte by the entrapped proteins is reversible or regenerable.

The function of entrapped enzymes has been probed using either fluorimetric substrates (i.e., acetylcholinesterase mediated catalysis of the reaction indoxyl acetate + H_2O → indoxyl + acetic acid, where only the product fluoresces)[90] or fluorescent coenzymes such as nicotinamide adenine dinucleotide phosphate ($NADP^+$ → NADPH or NAD^+ → NADH).[91,92] Entrapped antibody function has been examined by monitoring the binding of fluorescent probes to entrapped antidansyl[86] and antifluorescein[87] antibodies. In addition, our group has examined the function of entrapped Ca^{2+} binding proteins by monitoring either short-range energy transfer from a Trp residue in the protein binding loop to a bound lanthanide (using a site-directed mutant of rat oncomodulin)[81c] or the change in native Trp fluorescence obtained by a Ca^{2+}-induced conformational change in cod III parvalbumin on binding of the ligand.[81d] In all cases, the equilibrium binding constants dropped by 2−5 orders of magnitude upon entrapment and changed further both as a function of entrapment conditions and time after entrapment, generally becoming smaller at longer times. The large changes in the binding constants likely reflected electrostatic interactions between the negatively charged silicate matrix and the negatively charged groups in the proteins and may have also been partially determined by the differences in the properties of entrapped solvents as compared to bulk solvents.[93] The changes in protein function over time represent a major obstacle which remains to be overcome before viable sol−gel-based sensors with extended long-term stability can be produced.

A few studies (not based on fluorescence) have shown that protein function can be dramatically enhanced by incorporation of dopants into the glasses. Examples include the entrapment of atrazine chlorohydrolase into methyltrimethoxysilane-based materials,[94] the incorporation of lipase into polymer-doped materials formed from organically modified silanes (which produced an 8800% enhancement of activity compared to free lipase for esterification reactions[33,95]), the entrapment of glucose oxidase and horseradish peroxidase in the presence of a graft copolymer of polyvinylimidazole and polyvinylpyridine,[96] lactate oxidase and glycolate oxidase in the presence of charged polymers such as poly(vinylimidazole) and poly(ethyleneamine),[97] and the entrapment of acetylcholinesterase and butyrylcholinesterase in the presence of poly(ethylene glycol).[98] Such studies clearly demonstrate that polymer−protein interactions can be used advantageously to maximize protein stability and function; however, at present there is very limited information available on the mechanisms by which the stabilization is achieved. Clearly, there is a significant opportunity for fluorescence methods to shed light on the behavior of these biologically doped nanocomposites, and it is expected that such studies will soon appear.

7. Conclusions and Future Perspectives

This review has focused on the use of fluorescence probes and biomolecules to report on the local structure and dynamics of the microenvironment(s) within class I and class II sol−gel-derived nanocomposites. Overall, it is clear that detailed information is provided by entrapped fluorescent probes, including the evolution of solvent composition, pore structure, dopant dynamics, and homogeneity from the point of gelation up to the formation of the final materials. Such information can provide unique insights into the molecular level organization of the material, including the distribution of the organic material within the silica, the formation of self-assembled structures within molecularly templated materials, and the behavior of biomolecules entrapped within biocomposite materials.

While a significant body of information is now available on the properties of nanocomposite materials, more work is needed to determine the underlying mechanisms that result in the observed changes in polarity, pore structure, and dynamics and to understand the nature of the individual environments that contribute to heterogeneity in nanocomposites. Much of this work will require careful studies of how different probes sense the local microenvironments within identical materials and suggest that codoping of a single sample with multiple probes (that are separable spectroscopically) should be initiated to better understand the overall evolution of a given nanocomposite.

While fluorescence probe studies have given useful information on nanocomposites, it is important to recognize that most probes are small and hydrophobic and, thus, they tend to sequester into and therefore report from nonpolar regions within nanocomposites. Thus, the information gained is highly localized, and care must therefore be taken in interpreting the results of fluorescence studies. This is clearly demonstrated in the studies using 7AI in which limited solubility of the probe in water results in the adsorption of the probe to the silica matrix. The significant red-shift that is observed is no longer reporting on local solvent polarity, but rather on pore-wall composition. Failure to recognize this fact could lead to incorrect interpretations regarding solvent composition. It is therefore important to treat the results of a given fluorescence study in the context of other studies (NMR, IR, BET, etc.) on the same material, rather than interpreting them based on a single spectroscopic characteristic.

Overall, the ability to tune the properties of sol−gel-derived nanocomposites and to follow the results using fluorescence methods suggests that a number of potential applications are possible. For example, tuning the

polarity of the materials should provide for selective preconcentration of desired species, leading to better control over the properties of solid-phase microextraction coatings. The ability to tune the mobility of dopants and external reagents within the glass should lead to improved sensors with rapid response times and high sensitivity. The covalent attachment of fluorescent probes, either to the silane network or to dispersed polymers, leads to the potential for developing photonic devices with nonleachable dopants. Finally, the ability to control the internal environment can be advantageous in the realm of biologically doped silicates. Control over polarity and dynamics within such materials can be used to stabilize hydrophobic proteins, improve protein accessibility, and tune the association constants of entrapped proteins. Given the wide range of potential applications for selectively doped nanocomposites, it is clear that careful spectroscopic investigations of nanocomposites will continue to play an important role in the design and optimization of these materials.

References

(1) (a) Beecroft, L. L.; Ober, C. K. *Chem. Mater.* **1997**, *9*, 1302. (b) Levy, D. *Chem. Mater.* **1997**, *9*, 2666.
(2) Miller, R. D.; Hedrick, J. L.; Yoon, D. Y.; Cook, R. F.; Hummel, J. P. *Mater. Res. Soc. Bull.* **1997**, *10*, 44.
(3) Gbatu, T. P.; Sutton, K. L.; Caruso, J. A. *Anal. Chim. Acta* **1999**, *402*, 67.
(4) Lev, O.; Tsionsky, M.; Rabinovich, L.; Glezer, V.; Sampath, S.; Pankratov, I.; Gun, J. *Anal. Chem.* **1995**, *67*, 22A.
(5) Brinker, C. J.; Scherer, G. W. *Sol−Gel Science: The Physics and Chemistry of Sol−Gel Processing*; Academic Press: San Diego, 1990.
(6) Hench, L. L.; West. J. K. *Chem. Rev.* **1990**, *90*, 33.
(7) Avnir, D.; Braun, S.; Lev, O.; Ottolenghi, M. *Chem. Mater.* **1994**, *6*, 1605.
(8) Schubert, U.; Husing, N.; Lorenz, A. *Chem. Mater.* **1995**, *7*, 2010−2027.
(9) Babonneau, F.; Maquet, J. *Polyhedron* **2000**, *19*, 315.
(10) Deng, Q.; Moore, R. B.; Mauritz, K. A. *Chem. Mater.* **1995**, *7*, 2259.
(11) Colomban, P. *J. Raman Spectrosc.* **1996**, *27*, 747.
(12) Wall, G. C.; Brown, R. J. C. *J. Colloid Interface Sci.* **1981**, *82*, 141.
(13) Dahmouche, K.; Santilli, C. V.; Pulcinelli, S. H.; Craievich, A. F. *J. Phys. Chem. B* **1999**, *103*, 4937.
(14) Dunn, B.; Zink, J. I. *Chem. Mater.* **1997**, *9*, 2280.
(15) Stokes, G. G. *Philos. Trans. R. Soc. London* **1852**, *142*, 463.
(16) Lakowicz, J. R. *Principles of Fluorescence Spectroscopy*, 2nd ed.; Plenum Press: New York, 1999.
(17) *Topics in Fluorescence Spectroscopy*; Lakowicz, J. R., Ed.; Plenum Press: New York, 1991; Vol. 1: Techniques.
(18) *Topics in Fluorescence Spectroscopy*; Lakowicz, J. R., Ed.; Plenum Press: New York, 1991; Vol. 2: Principles.
(19) *Topics in Fluorescence Spectroscopy*; Lakowicz, J. R., Ed.; Plenum Press: New York, 1991; Vol. 3: Biochemical Applications.
(20) *Topics in Fluorescence Spectroscopy*; Lakowicz, J. R., Ed.; Plenum Press: New York, 1994; Vol. 4: Probe Design and Chemical Sensing.
(21) Haugland, R. P. *Molecular Probes Catalog*, Eugene, OR, 1996.
(22) Narang, U.; Jordan, J. D.; Bright, F. V.; Prasad, P. N. *J. Phys. Chem.* **1994**, *98*, 8101.
(23) (a) Matsui, K.; Matsuzuka, T.; Fujita, H. *J. Phys. Chem.* **1989**, *93*, 4991. (b) Flora K. K.: Dabrowski, M. A.; Musson, S. P.; Brennan, J. D. *Can. J. Chem.* **1999**, *77*, 1617.
(24) Kikteva, T. A.; Snmud, B. V.; Smirnova, N. P.; Eremenko, A. M.; Polevaya, Y.; Ottolenghi, M. *J. Colloid Interface Sci.* **1997**, *193*, 163.
(25) McKiernan, J.; Pouxviel, J. C.; Dunn, B.; Zink, J. I. *J. Phys. Chem.* **1989**, *93*, 2129.
(26) Black, I.; Birch, D. J. S.; Ward, D.; Leach, M. J. *J. Fluoresc.* **1997**, *7*, 111S.
(27) (a) Narang, U.; Wang, R.; Prasad, P. N.; Bright, F. V. *J. Phys. Chem.* **1994**, *98*, 17. (b) Gottfried, D. S.; Kagan, A.; Hoffman, B. M.; Friedman, J. M. *J. Phys. Chem. B* **1999**, *103*, 2803. (c) Qian, G.; Minquan, W. *J. Phys. D: Appl. Phys.* **1999**, *32*, 2462. (d) L'Esperance, D.; Chromister, E. L. *Chem. Phys. Lett.* **1994**, *222*, 217.
(28) Meneses-nava, M. A.; Chavez Cerda, S.; Sanchez-Villicana, V.; Sanchez-Mondragon, J. J.; King, T. A. *Mex. Opt. Mater.* **1999**, *12*, 441.
(29) (a) Samuel, J.; Polevaya, Y.; Ottolenghi, M.; Avnir, D. *Chem. Mater.* **1994**, *6*, 1457. (b) Bonzagni, N. J.; Baker, G. A.; Pandey, S.; Niemeyer, E. D.; Bright, F. V. *J. Sol-Gel Sci. Technol.* **2000**, *17*, 83.
(30) (a) Shen, C.; Kostic, N. M. *J. Am. Chem. Soc.* **1997**, *119*, 1304. (b) Zheng, L.; Reid, W. R.; Brennan, J. D. *Anal. Chem.* **1997**, *69*, 3940.
(31) Avnir, D.; Klein, L. C.; Levy, D.; Schubert, U.; Wojcik, A. B. In *The Chemistry of Organic Compounds*; Rappoport, Z., Apeloig, Y., Eds.; Wiley: New York, 1998.
(32) Baker, G. A.; Pandey, S.; Maziarz, E. P., III.; Bright, F. V. *J. Sol-Gel Sci. Technol.* **1999**, *15*, 37.
(33) Brennan, J. D.; Hartman, J. S.; Ilnicki, E. I.; Rakic, M. *Chem. Mater.* **1999**, *11*, 1853.
(34) Matsui, K.; Tominaga, M.; Arai, Y.; Satoh, H.; Kyoto, M. *J. Non-Cryst. Solids* **1994**, *169*, 295.
(35) Lobnik, A.; Wolfbeis, O. S. *Analyst* **1998**, *123*, 2247.
(36) Wong, A. L.; Hunnicutt, M. L.; Harris, J. M. *Anal. Chem.* **1991**, *63*, 1076.
(37) Dong, D. C.; Winnik, M. *Photchem. Photobiol.* **1982**, *35*, 17.
(38) Weber G.; Farris, F. J. *Biochemistry* **1979**, *18*, 3075.
(39) (a) Chapman, C. F.; Maroncelli, M. *J. Phys. Chem.* **1992**, *96*, 8430. (b) Rich, R. L.; Chen, Y.; Neven, D.; Negerie, M.; Gai, F.; Petrich, J. W. *J. Phys. Chem.* **1993**, *97*, 1781.
(40) Sun, S.; Heitz, M. P.; Perez, S. A.; Colon, L. A.; Bruckenstein, S.; Bright, F. V. *Appl. Spectrosc.* **1997**, *51*, 1316.
(41) Wittouck, N.; De Schryver, F.; Snijkers-Hendrickx, I. *J. Sol-Gel Sci. Technol.* **1997**, *8*, 895.
(42) Pines, E.; Huppert, D. *J. Phys. Chem.* **1983**, *87*, 4471.
(43) Kaufman, V. R.; Avnir, D.; Pines, D.; Huppert, D. *J. Non-Cryst. Solids* **1988**, *99*, 379.
(44) McDonagh, C.; MacCraith, B. D.; McEvoy, A. K. *Anal. Chem.* **1998**, *70*, 45.
(45) Murtagh, M. T.; Kwon, H. C.; Shahriari, M. R. *Proc. SPIE−Int. Soc. Opt. Eng.* **1997**, *3136*, 187.
(46) Zhang, Y.; Wang, M. *Mater. Lett.* **2000**, *42*, 86.
(47) Chambers, R. C.; Haruvy, Y.; Fox, M. A. *Chem. Mater.* **1994**, *6*, 1351.
(48) Pandey, S.; Baker, G. A.; Kane, M. A.; Bonzagni, N. J.; Bright, F. V. *Chem. Mater.* **2000**, *12*, 3547.
(49) Gvishi, R.; Narang, U.; Bright, F. V.; Prasad, P. N. *Chem. Mater.* **1995**, *7*, 1703.
(50) Ilharco, L. M.; Martinho, J. M. G. *Langmuir* **1999**, *15*, 7490.
(51) Leezenberg, P. B.; Frank, C. W. *Chem. Mater.* **1995**, *7*, 1784.
(52) Meech, S. R.; O'Connor, D. V.; Phillips, D. *J. Chem. Soc., Faraday Trans. 2* **1983**, *79*, 1563.
(53) Baker, G.A.; Jordan, J. D.; Bright, F. V. *J. Sol-Gel Sci. Technol.* **1998**, *11*, 43.
(54) Lesot, P.; Chapuis, S.; Bayle, J. P.; Rault, J.; Lafontaine, E.; Campero, A.; Judeinstein, P. *J. Mater. Chem.* **1998**, *8*, 147.
(55) Keeling-Tucker, T.; Rakic, M.; Spong, C.; Brennan, J. D. *Chem. Mater.* **2000**, *12*, 3695.
(56) Reetz, M. T.; Zonta, A.; Simpelkamp, J. *Biotechnol. Bioeng.* **1996**, *49*, 527.
(57) Gill, I.; Ballesteros, A. *J. Am. Chem. Soc.* **1998**, *120*, 8587.
(58) Wang, B.; Li, B.; Deng, Q.; Dong, S. *Anal. Chem.* **1998**, *70*, 3170.
(59) Baker, G. A.; Watkins, A. N.; Pandey, S.; Bright, F. V. *Analyst* **1999**, *124*, 373.
(60) Stathatos, E.; Lianos, P.; Stangar, U. L.; Orel, B.; Judeinstein, P. *Langmuir* **2000**, *16*, 8672.
(61) del Monte, F.; Levy, D. *J. Sol-Gel Sci. Technol.* **1997**, *8*, 585.
(62) del Monte, F.; Ferrer, M. L.; Levy, D. *J. Mater. Chem.* **2001**, *11*, Advance Article b009403.
(63) Deng, Q.; Hu, Y.; Moore, R. B.; McCormick, C. L.; Mauritz, K. A. *Chem. Mater.* **1997**, *9*, 36.
(64) Deng, Q.; Moore, R. B.; Mauritz, K. A. *Chem. Mater.* **1995**, *7*, 2259.
(65) Mauritz, K. A. *Mater. Sci. Eng. C* **1998**, *6*, 121.
(66) Carr, S. W.; Courtney, L.; Sullivan, A. C. *Chem. Mater.* **1997**, *9*, 1751.
(67) Wei, Y.; Jin, D. L.; Ding, T. Z.; Shih, W. H.; Liu, X. H.; Cheng, S. Z. D. *Adv. Mater.* **1998**, *10*, 313.
(68) Sanchez, C.; Lebeau, B.; Ribot, F.; In, M. *J. Sol-Gel Sci. Technol.* **2000**, *19*, 31.
(69) Bekiari, V.; Ferrer, M.; Stathatos, E.; Lianos, P. *J. Sol-Gel Sci. Technol.* **1998**, *13*, 95.
(70) Bekiari, V.; Ferrer, M.-L.; Lianos, P. *J. Phys. Chem. B* **1999**, *103*, 9085.
(71) Lu, Y.; Ganguli, R.; Drewien, C. A.; Anderson, M. T.; Brinker, C. J.; Gong, W.; Guo, Y.; Soyez, H.; Dunn, B.; Huang, M. H.; Zink, J. I. *Nature* **1997**, *389*, 364.
(72) Nishida, F.; McKiernan, J. M.; Dunn, B.; Zink, J. I.; Brinker, C. J.; Hurd, A. J. *J. Am. Ceram. Soc.* **1995**, *78*, 1640.
(73) Chia, S.; Huang, M. H.; Dunn, B. S.; Soyez, H.; Zink, J. I. *Langmuir* **1998**, *14*, 7331.

(74) Huang, M. H.; Dunn, B. S.; Zink, J. I. *J. Am. Chem. Soc.* **2000**, *122*, 3739.
(75) Chia, S.; Urano, J.; Fuyuhiko, T.; Dunn, B.; Zink, J. I. *J. Am. Chem. Soc.* **2000**, *122*, 6488.
(76) Hernandez, R.; Franville, A.-C.; Minoofar, P.; Dunn, B.; Zink, J. I. *J. Am. Chem. Soc.* **2001**, *123*, 1248.
(77) Katz, A.; Davis, M. E. *Nature* **2000**, *403*, 286.
(78) Yamanaka, S. A.; Charych, D. H.; Loy, D. A.; Sasaki, D. Y. *Langmuir* **1997**, *13*, 5049.
(79) Nguyen, T.; McNamara, K. P.; Rosenweig, Z. *Anal. Chim. Acta* **1999**, *400*, 45.
(80) Edmiston, P. L.; Wambolt, C. L.; Smith, M. K.; Saavedra, S. S. *J. Colloid Interface Sci.* **1994**, *163*, 395.
(81) (a) Zheng, L.; Reid, W. R.; Brennan, J. D. *Anal. Chem.* **1997**, *69*, 3940. (b) Zheng, L.; Brennan, J. D. *Analyst* **1998**, *123*, 1735. (c) Zheng, L.; Flora, K.; Brennan, J. D. *Chem. Mater.* **1998**, *10*, 3974. (d) Flora, K.; Brennan, J. D. *Anal. Chem.* **1998**, *70*, 4505. (e) Brennan, J. D. *Appl. Spectrosc.* **1999**, *53*, 106A.
(82) Stewart, C. A.; Vanderkooi, J. M. *J. Floresc.* **1999**, *9*, 89.
(83) Ellerby, L.; Nishida, C.; Nishida F.; Yamanka S.; Dunn, B.; Valentine, J. S.; Zink, J. I. *Science* **1992**, *255*, 1113.
(84) Jordan, J. D.; Dunbar, R. A.; Bright, F. V. *Anal. Chem.* **1995**, *67*, 2436.
(85) Gottfried. D. S.; Kagan, A.; Hoffman, B. M.; Friedman, J. M. *J. Phys. Chem. B* **1999**, *103*, 2803.
(86) Doody, M. A.; Baker, G. A.; Pandey, S.; Bright, F. V. *Chem. Mater.* **2000**, *12*, 1142.
(87) Wang, R.; Narang, U.; Prasad, P. N.; Bright, F. V. *Anal. Chem.* **1993**, *65*, 2671.
(88) Samuni, U.; Navati, M. S.; Juszczak, L. J.; Dantsker, D.; Yang, M.; Friedman, J. M. *J. Phys. Chem. B* **2000**, *104*, 10802.
(89) Wambolt, C. L.; Saavedra, S. S. *J. Sol-Gel Sci. Technol.* **1996**, *7*, 53.
(90) Diaz, A. N.; Peinado, M. C. R. *Sensors Actuators B* **1997**, *38*−*39*, 426.
(91) Williams, A. K.; Hupp, J. T. *J. Am. Chem. Soc.* **1998**, *120*, 4366.
(92) Yamanaka, S. A.; Dunn, B.; Valentine, J. S.; Zink, J. I. *J. Am. Chem. Soc.* **1995**, *117*, 9095.
(93) (a) Korb, J.-P.; Delville, A.; Xu, S.; Demeulenaere, G.; Costa, P.; Jonas, J. *J. Chem. Phys.* **1994**, *101*, 7074. (b) Xu, S.; Ballard, L.; Kim, J.; Jonas, J. *J. Phys. Chem.* **1995**, *99*, 5787.
(94) Kauffmann, C.; Mandelbaum, R. T. *J. Biotechnol.* **1998**, *62*, 169.
(95) (a) Reetz, M. T.; Zonta, A.; Simpelkamp, J.; Konen, W. *Chem. Commun.* **1996**, 1397. (b) Reetz, M. T.; Zonta, A.; Simpelkamp, J. *Angew. Chem., Int. Ed. Engl.* **1995**, *34*, 301. (c) Kuncova, G.; Guglielmi, M.; Dubina, P.; Safar, B. *Collect. Czech. Chem. Commun.* **1995**, *60*, 1573.
(96) (a) Wang, B.; Li, B.; Deng, Q.; Dong, S. *Anal. Chem.* **1998**, *70*, 3170. (b) Wang, B.; Li, B.; Wang, Z.; Xu, G.; Wang, Q.; Dong, S. *Anal. Chem.* **1999**, *71*, 1935.
(97) (a) Chen, Q.; Kenausis, G. L.; Heller, A. *J. Am. Chem. Soc.* **1998**, *120*, 4582. (b) Heller, J.; Heller, A. *J. Am. Chem. Soc.* **1998**, *120*, 4586.
(98) Altstein, M.; Segev, G.; Aharonson, N.; Ben-Aziz, O.; Turniansky, A.; Avnir, D. *J. Agric. Food Chem.* **1998**, *46*, 3318.

CM010119M